UNIVERSITY OF CHEMICAL TECHNOLOGY AND METALLURGY
FACULTY OF METALLURGY AND MATERIALS SCIENCE
DEPARTMENT OF PHYSICAL METALLURGY AND HEAT AGGREGATES

Nikita Alexandrovich Lutchenko

ABSTRACT

of the dissertation

Investigation of the possibility of obtaining an ultrafine-grained structure of zirconium alloys by methods of intensive plastic deformation

for acquiring the educational and scientific degree "Doctor" (PhD)
in science 5.6 Materials and Materials Science
(Materials science and technology of engineering materials)

Scientific Supervisors:
Prof. Eng. R.M. Yordanova, PhD
A.S. Arbuz, PhD

The composition of the scientific council:

1. Prof. Eng. E. Mihailov, PhD - chairman, reviewer
2. Prof. Eng. S. Gyurov, PhD - reviewer
3. Assoc. Prof. Eng. D. Grigorova, PhD
4. Prof. Eng. R. Lazarova, PhD
5. Prof. Eng. A. Velikov, PhD

Sofia, 2025

The dissertation is written on 174 pages, contains 113 figures and 9 tables. There are 270 references.

The presented dissertation was discussed and accepted for defense at a meeting of the Scientific Council of the scientific unit of the Department "physical metallurgy and thermal aggregates", held on 27.11.2025.

The public defense of the dissertation will be held on 00.00.2025. from 00:00 in Hall 301, Building" A " of UCTM.

The materials are available to those interested on the website of UCTM and in the "scientific activities" Department, Room 406, floor 4, Building "A" of UCTM.

List of abbreviations

ADS	–	Accelerator Driven Systems
ARB	–	Accumulative Roll Bonding
ASTM	–	American Society for Testing and Materials
BF	–	Bright Field
BWR	–	Boiling Water Reactor
CAD	–	Computer-Aided Design
CANDU	–	Canada Deuterium Uranium
CEC	–	Cyclic Extrusion Compression
CEE	–	Cyclic Expansion-Extrusion
DOE	–	Design of Experiments
EBSD	–	Electron Backscatter Diffraction
ECAD	–	Equal Channel Angular Drawing
ECAE	–	Expansion equal channel angular extrusion
ECAP	–	Equal Channel Angular Pressing
ECAS	–	Equal channel angular swaging
FA	–	Fuel Assembly
FEM	–	Finite Elements Method
HALEU	–	High-Assay Low-Enriched Uranium
HANA	–	High performance Alloy for Nuclear Application
HCP	–	Hexagonal Close Packed
HPT	–	High Pressure Torsion
HTGR	–	High-Temperature Gas-cooled Reactor
HTR-PM	–	High-Temperature gas-cooled Reactor Pebble-bed Module
IAEA	–	International Atomic Energy Agency
IPF	–	Inverse Pole Figures
LOCA	–	Loss-Of-Coolant Accident
LWR	–	Light Water Reactors
MDA	–	Mitsubishi Developed Alloy
MDF	–	Multi-Directional Forging
NDA	–	New Developed Alloy
NPP	–	Nuclear Power Plant
ODF	–	Orientation Distribution Function
PCMI	–	Pellet-cladding mechanical interaction
PCMI- SCC	–	Pellet-cladding interaction-stress corrosion cracking
PHWR	–	Pressurised Heavy Water Reactor
PWR	–	Pressurized Water Reactor
RSR	–	Radial Shear Rolling
RXA	–	Recrystallized Annealed
SIPA	–	Stress Induced Preferential Absorption
SMR	–	Small Modular Reactor
SPD	–	Severe Plastic Deformation
SPP	–	Secondary Phase Particles
SRA	–	Stress-Relieved Annealed
TCAP	–	Twist channel angular pressing
TE	–	Twisty Extrusion
TEM	–	Transmission electron microscopy
UFG	–	Ultrafine-Grained
VVER	–	from Russian: Vodo-Vodyanoi Enyergeticheskiy Reaktor
WWER	–	Water-Water Energetic Reactor
XRD	–	X-ray Diffraction

INTRODUCTION AND RELEVANCE OF THE RESEARCH TOPIC.

Modern energy systems require technologies that combine high efficiency, safety, and environmental sustainability. Against the backdrop of global population growth and accelerating electrification, the transition toward sustainable energy sources has become particularly relevant. Among these, nuclear energy occupies a key position due to its ability to provide stable power generation with a minimal carbon footprint.

The reliability of nuclear reactors is largely determined by the properties of structural materials, particularly the fuel cladding, which operates under conditions of high temperature, pressure, and intense radiation. The main challenges associated with the operation of zirconium alloys include the degradation of their properties, radiation-induced growth, creep, hydrogen embrittlement, and crack formation.

Zirconium alloys have traditionally been used in nuclear reactors due to their low thermal neutron absorption cross-section, corrosion resistance, and mechanical strength. However, their service properties deteriorate over time. In this regard, there has been growing interest in the development of ultrafine-grained (UFG) and nanostructured materials, which provide enhanced strength, hardness, fatigue resistance, and radiation tolerance. These improvements are attributed to the high density of grain boundaries that effectively trap radiation-induced defects and reduce the likelihood of dislocation loop formation and microcrack propagation.

In addition to grain size, the crystallographic texture plays a crucial role in determining the anisotropy of properties in zirconium, which has a hexagonal close-packed (HCP) crystal structure. Controlling the texture allows for the reduction of radiation-induced growth and improvement of the service life of fuel claddings. To achieve this, various Severe Plastic Deformation (SPD) techniques are employed, such as equal channel angular pressing (ECAP), high-pressure torsion (HPT), and, in particular, Radial-Shear rolling (RSR).

Radial-Shear rolling (RSR) stands out by combining intense grain refinement with the capability of processing long-length billets, which makes this method highly promising for the fabrication of nuclear fuel claddings. The process generates a complex stress–strain state, promotes the formation of a gradient ultrafine-grained (UFG) structure, and contributes to the development of a favorable crystallographic texture.

Thus, the study of the application of RSP to zirconium alloys for the formation of the UFG structure and improvement of mechanical properties, texture and radiation resistance is an urgent scientific and applied task that meets the requirements of modern nuclear energy.

RESEARCH OBJECTIVES AND TASKS OF THE DISSERTATION.

– To analyze the modern requirements for structural materials used in the reactor core and to identify the key mechanisms of their degradation under irradiation, as well as to assess the feasibility of applying ultrafine-grained (UFG) structures based on zirconium alloys;

– To summarize and classify the existing methods for obtaining UFG structures and evaluate their applicability to zirconium alloys, taking into account scalability, product geometry, and operating conditions in nuclear reactors;

– To develop a technological scheme of radial-shear rolling (RSR) using finite element modeling (FEM) of the process, to investigate the features and regularities of the stress–strain state of zirconium, and to optimize the geometric and technological parameters of rolling;

– To carry out a series of experimental RSR trials and obtain billets of various diameters for analyzing the evolution of the resulting structure;

– To investigate the microstructural evolution across the cross-section of the billets obtained by RSR using transmission and scanning electron microscopy, including EBSD mapping, and to perform an analysis of texture characteristics (including the calculation of Kearns parameters);

– To study the fine structure of samples produced by radial-shear rolling using high-resolution electron microscopy;

– To obtain data on their mechanical properties;

– To conduct heavy-ion irradiation of the samples in order to simulate damage conditions caused by fission fragments in the reactor core.

METHODOLOGY AND RESEARCH METHODS.

Both theoretical and experimental scientific research methods were employed in this project. The classical theoretical methods included analysis of scientific and patent literature, experimental design, and statistical processing of experimental data. Additionally, finite element modeling (FEM) was used to analyze the stress–strain state during the development of the radial-shear rolling technology for zirconium. This method was applied to optimize the processing parameters for producing ultrafine-grained (UFG) zirconium and was implemented using the DEFORM-3D software package (Scientific Forming Technologies Corporation, USA). Subsequently, the same finite element approach was utilized to predict the behavior of structural components made from the obtained UFG zirconium.

The complete geometric models were constructed using the CAD software KOMPAS-3D (ASCON, Russia) with the APM-Expert module. The experimental production of ultrafine-grained zirconium was carried out on Radial-Shear Rolling mills RSP-14/30 (also known as SVP-08) at Rudny Industrial Institute and RSP-10/30 at Karaganda Industrial Institute.

The mechanical properties were evaluated using standard tensile tests performed on an Instron testing machine (USA) and by measuring the Vickers microhardness (HV) with a Shimadzu HMV-G31ST microhardness tester.

A part of the rheological studies required for constructing computational models was carried out on a Gleeble-3800-GTC plastometer (Dynamic Systems Inc., USA) at the Częstochowa University of Technology (Poland). The changes in the phase composition of the samples were analyzed using X-ray diffraction (XRD) on a Rigaku SmartLab diffractometer (Japan).

The microstructural characterization of the samples will be carried out using high-resolution scanning and transmission electron microscopy on the following instruments: Zeiss CrossBeam 540 field-emission scanning electron microscope (Germany), a JEOL JSM-IT200LA scanning electron microscope (Japan), and a JEOL JEM-1400PLUS transmission electron microscope (Japan).

For specimen preparation, in addition to standard cutting and grinding machines, electrolytic polishing and thinning will be performed using TenuPol-5 and LectroPol-5 systems (Struers, Denmark).

The study of radiation resistance and defect formation processes under irradiation will be conducted using the DC-60 accelerator complex at the Astana branch of the Institute of Nuclear Physics of the National Nuclear Center of the Republic of Kazakhstan (NNC RK).

1 1 Technologies for the Production and Prospects of Ultrafine-Grained Materials in Nuclear Energy.

1.1 Nuclear energy materials. Main requirements and development trends.

Global energy consumption has shown steady growth, increasing from 20,000 TWh in 1965 to over 160,000 TWh in 2021. The main contribution to this growth comes from developing countries, although developed economies have also increased their energy demand through the electrification of industry and transport. Despite the rising share of renewable energy sources, oil and coal continue to dominate the global energy mix, while the expansion of intermittent renewables (such as solar and wind) remains constrained by stability issues, grid balancing challenges, and high infrastructure costs.

Under these conditions, nuclear power gains particular importance as a source of low-carbon and stable energy supply. Currently, more than 400 reactors are in operation worldwide, with over 80% being light-water reactors (LWRs). Nuclear energy demonstrates a high level of safety: over more than 60 years of operation, only three major accidents have been recorded, making it statistically one of the safest energy industries. Modern advancements focus on risk reduction through the development of Generation IV reactors, small modular reactors (SMRs), and closed fuel cycle technologies, which aim to enhance sustainability, resource efficiency, and long-term safety of nuclear power systems.

A key direction of progress in nuclear energy remains the management and reduction of radioactive waste. Ongoing research focuses on the use of fast reactors, accelerator-driven systems (ADS), and transmutation technologies, which significantly reduce the long-term radiotoxicity of nuclear waste. Small modular reactors (SMRs), due to their modular design, operational flexibility, and inherent passive safety features, exhibit strong potential for widespread deployment in the coming decades, contributing to the diversification and decentralization of nuclear energy production.

The reliability of nuclear power is determined by the quality of structural materials. In the reactor core, these materials must withstand high temperatures (up to 350 °C under normal conditions and over 900 °C during LOCA accidents), high

pressures (70–155 bar), and intense neutron fluxes (~10^{13}–10^{15} n/cm^2·s). The most critical materials are those used for fuel rod claddings, where zirconium alloys are traditionally employed due to their low neutron absorption cross-section, corrosion resistance, and satisfactory mechanical properties.

Since the 1950s, a wide range of zirconium alloys has been developed—Zircaloy-2, Zircaloy-4, E110, E125, E635, ZIRLO, M5, and others—differing in their alloying with Sn, Nb, Fe, Cr, Ni, and other elements. Various countries are working on new compositions (such as NDA, MDA, HANA, AXIOM, etc.); however, their implementation requires verification of operational advantages. Current trends show a gradual transition away from Zircaloy-4 toward alloys such as E110, E635, ZIRLO, and M5, which offer higher corrosion resistance, improved resistance to hydrogen embrittlement, and better performance under elevated temperature and fuel burnup conditions.

Thus, the development of nuclear energy is closely linked to the improvement of structural materials, particularly zirconium alloys, which remain the foundation for enhancing the reliability and safety of modern and next-generation reactors.

1.2 Defects, Damage, and Irradiation Effects in Zirconium Alloy Nuclear Claddings.

One of the key factors determining the operational reliability of nuclear fuel is the resistance of zirconium claddings to various types of degradation caused by mechanical, chemical, and radiation effects. Primary mechanical defects include wear mechanisms such as grid-to-rod fretting and debris-fretting, as well as pellet–cladding mechanical interaction (PCMI) and the associated processes of pellet–cladding interaction stress corrosion cracking (PCI-SCC). These defects arise from vibrations of fuel rods, contact with support structures within the assembly, the presence of foreign particles in the coolant, and the stressed interaction between the fuel pellet and the zirconium cladding during power changes. The consequences of these processes manifest as local material wear, coolant ingress into the fuel rod, and the initiation of crack formation.

Corrosion-related damage includes localized degradation zones caused by violations of the water–chemistry regime or exposure to aggressive fission products. Hydrogen accumulation in the material plays a significant role, as it leads to the formation of brittle zirconium hydrides and the development of hydride cracking. Secondary defects—such as hydride blisters, internal corrosion zones, microcracks, and local ruptures—form as a result of coolant penetration through primary damage sites.

Radiation effects play a fundamental role in the degradation of fuel claddings. Irradiation by fast neutrons and gamma rays initiates the formation of point defects, dislocation loops, and vacancy clusters, which lead to radiation hardening, growth, and creep. Radiation hardening increases the material's strength but reduces its ductility, thereby increasing the risk of brittle fracture. Radiation growth manifests as anisotropic deformation caused by the hexagonal crystal lattice of zirconium,

resulting in geometric changes of the fuel elements. Creep under irradiation further exacerbates deformation, reducing operational reliability.

A key factor determining the durability of zirconium claddings is the crystallographic texture formed during thermo-mechanical processing. The orientation of basal planes governs the material's susceptibility to radiation growth, creep, and hydride formation. To quantitatively assess anisotropy, the Kearns parameter is used—it characterizes the distribution of grain orientations and allows prediction of the cladding's operational behavior. Studies show that optimizing texture and grain size is one of the most effective means of improving the radiation resistance of zirconium alloys.

Thus, the combined influence of mechanical, corrosion-related, and radiation-induced defects determines the overall reliability of fuel rod claddings. Minimizing these processes requires a scientifically grounded approach to selecting the composition, microstructure, and texture of zirconium alloys—an essential strategic objective for the further advancement of nuclear energy.

1.3 Ultrafine-Grained Materials: Their Characteristics and Prospects for Application in Nuclear Energy.

One of the most promising approaches to improving the performance of structural materials for nuclear power applications is the use of ultrafine-grained (UFG) and nanostructured (NS) states. In zirconium alloys, which are traditionally used as fuel rod cladding materials, the typical grain size ranges from 5 to 20 μm. The formation of a grain structure with a characteristic size below 1 μm, however, can significantly alter both the mechanical and radiation properties of the material.

UFG materials exhibit enhanced strength due to grain boundary strengthening, described by the Hall–Petch mechanism. When transitioning to the nanoscale level (<100 nm), additional mechanisms come into play: intergranular sliding, the active participation of grain boundaries as sources and sinks for dislocations, and the formation of nonequilibrium grain boundaries. Such structures provide a combination of high strength and acceptable ductility immediately after processing, making them highly attractive for nuclear technology applications (Figure 1).

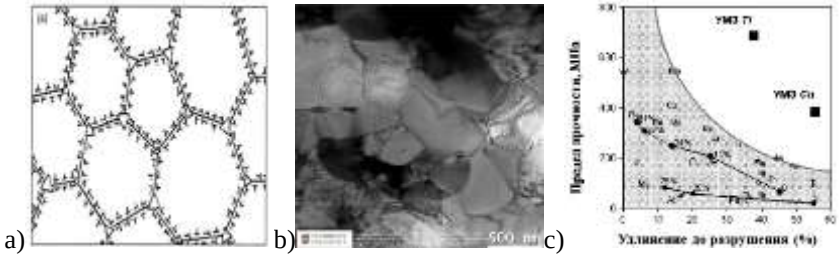

Figure 1 - Features of ultrafine-grained (UFG) materials.
a) Schematic representation of the structure of an ultrafine-grained (UFG) metal; b) TEM image of the UFG zirconium structure; c) Mechanical properties of conventional and UFG structural states for various metals

A key factor in improving radiation resistance in UFG and NS materials is the high density of grain boundaries, which act as effective sinks for radiation-induced defects. This enhances the rate of defect annihilation and reduces the likelihood of damage accumulation that leads to embrittlement and swelling of the material. Such effects have been experimentally confirmed not only in zirconium alloys but also in austenitic steels, where grain refinement has been shown to reduce the degree of amorphization and radiation hardening.

Global research in this field is actively progressing in leading nuclear research centers in the United States, France, Japan, and other countries, demonstrating the high level of international interest in this promising direction.

1.4 Existing methods for producing ultrafine-grained (UFG) materials.

To enhance the strength and radiation resistance of materials, the formation of ultrafine-grained (UFG) and nanostructured (NS) states is a promising strategy. Classical approaches—such as rapid solidification (melt spinning, gas atomization, spray forming), additive manufacturing (SLM/EBM), chemical synthesis (sol–gel), and powder metallurgy—are effective for producing powders, thin films, and complex geometries, but they have limitations when applied to large-scale, elongated metallic components such as fuel cladding tubes.

Rapid solidification primarily yields powders or foils and poses significant challenges in precise property control. Additive processes are limited by build rate, component size, and high cost. The sol–gel method is time-consuming, material-intensive, and better suited for oxides rather than metals. Powder metallurgy, meanwhile, suffers from residual porosity and the high cost of initial powders, which reduces ductility and toughness and complicates large-scale industrial implementation.

The most suitable platform for producing bulk billets with a homogeneous ultrafine-grained (UFG) structure is severe plastic deformation (SPD) methods. These techniques eliminate the porosity inherent to sintering but require adherence to several key conditions:

(I) an accumulated strain of $\varepsilon > 6–8$;

(II) a high level of hydrostatic pressure (≈ GPa) to prevent fracture and defect relaxation;

(III) a deformation temperature $\lesssim 0.3\ T$□ for Zr alloys—below the $\alpha \rightarrow \alpha + \beta$ transition range;

(IV) a nonmonotonic or turbulent deformation path to promote the formation of high-angle grain boundaries.

The more completely these conditions are satisfied, the faster and more uniformly a UFG state is formed.

Among the most extensively studied SPD processes are: HPT (High-Pressure Torsion) — used to produce disk-shaped samples with extreme grain refinement; ARB (Accumulative Roll Bonding) — involves repeated rolling of stacked sheets with interlayer bonding and strain accumulation in the material; MDF (Multi-Directional Forging) — alternating compression along several axes for bulk billets;

CEC (Cyclic Extrusion Compression) — repeated passes through a die with back pressure while maintaining the sample's overall dimensions; ECAP/ECAE (Equal Channel Angular Pressing/Extrusion) — pressing through a die with equal cross-sections and specific rotation routes, scalable to centimeter-sized billets and partially implemented at the industrial level.

Despite the high scientific maturity of the aforementioned approaches, their widespread industrial application remains limited by several factors:

– the complexity and cost of specialized tooling and precise process control;

– geometric and dimensional constraints (often limited to small disks or billets, with difficulties in processing long components);

– high force and energy requirements, as well as limited tool lifetime.

These barriers are particularly critical for long, hollow, or solid components such as nuclear fuel cladding tubes, where process continuity, high productivity, and structural uniformity along the entire length are essential.

Given these requirements, a justified transition can be made toward Radial-Shear Rolling (RSR) as an SPD variant specifically suited for long, round billets. RSR provides intense gradient shear deformation under substantial triaxial compression, is compatible with conventional rolling lines, and is technologically closer to industrial processing routes. It enables the production of UFG states in rods (and tube preforms) with controllable structural gradients across the cross-section. This approach creates a foundation for scalable fabrication of radiation-resistant UFG zirconium semifinished products and for the subsequent adaptation of the technology to the industrial production of nuclear fuel cladding components.

1.5 Radial-Shear Rolling Technology for Producing Long-Length Ultrafine-Grained Materials.

Radial-shear rolling is a type of helical rolling process used for solid billets on a three-roll mill. Fundamentally, the process is similar to tube piercing technology but differs in that it employs three specially calibrated rolls (Figure 2) instead of two, along with larger feed angles (18–25°). Unlike conventional piercing, where small feed angles lead to the Mannesmann effect and the formation of an axial cavity, radial-shear rolling densifies the material throughout the entire cross-section, preventing internal damage even under large reductions.

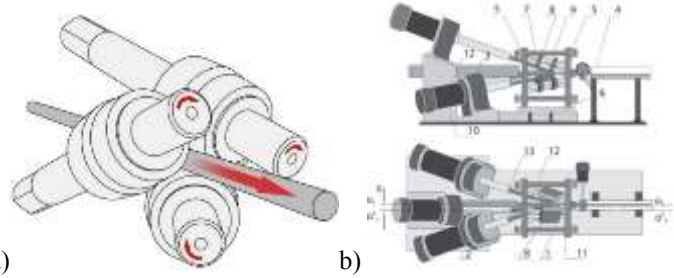

a) b)

Figure 2 - a) Radial-shear rolling scheme b) Principal arrangement of RSR mini mill.

The main feature of the process is the combination of triaxial compression and intense shear deformation, accompanied by turbulent metal flow within the deformation zone. This complex stress–strain state generates a pronounced gradient of flow velocities and directions across the billet radius, resulting in the elongation, refinement, and high dispersion of structural elements. The outer layers of the billet experience alternating compression and tension along a helical trajectory, creating favorable conditions for the formation of isotropic fine-dispersed particles and a characteristic banded structure.

An important feature of radial-shear rolling is the nonmonotonic and multi-path nature of the deformation trajectories. This promotes the formation of high-angle grain boundaries, which are essential for achieving ultrafine-grained (UFG) states. In its characteristics, the process combines elements of both longitudinal rolling and extrusion, ensuring thorough structural refinement throughout the entire volume of the billet.

For practical applications, compact rolling mills with small working diameters have been developed, enabling the processing of billets ranging from 10 to 40 mm in diameter. These installations implement different roll adjustment schemes (axial or radial), allow for multistage rolling, and provide flexibility in controlling process parameters. This approach makes it possible to produce long rods with a controlled ultrafine-grained (UFG) structure, with the final product length limited only by the specific capabilities of the rolling mill.

It can be concluded that radial-shear rolling most effectively meets the key requirements of severe plastic deformation (SPD) methods: it provides large accumulated strains, a high level of triaxial compression, turbulent material flow, and the capability to process long billets. This makes it a promising tool for producing ultrafine-grained (UFG) structures in zirconium alloys intended for nuclear fuel cladding applications, underscoring the high scientific and practical significance of further research in this field.

2 Computer-based modeling and process development for producing ultrafine-grained zirconium using radial-shear rolling.

2.1 Plastometric studies of the rheological behavior of zirconium and the development of a material database for computer-based modeling.

To study the characteristics of the radial-shear rolling process, the Deform software–based on the finite element method–was used. The design of the SVP-08 (RSR-14/30) rolling mill served as the prototype. A billet with a diameter of 37 mm and a length of 150 mm was modeled at a heating temperature of 530 °C, which prevents phase transformations in the alloy. The roll rotation speed was set to 100 rpm, and the friction coefficient at the billet–roll interface was assumed to be 0.7 (according to the Siebel model), corresponding to the conditions of hot deformation under high contact pressure.

The simulation was carried out in a non-isothermal mode, with simultaneous solution of the mechanical and thermal problems. Heat transfer coefficients were specified for the billet's interaction with both the environment and the tooling. The

roll geometry was designed in KOMPAS-3D and imported into Deform in STL format. The rolls were modeled as absolutely rigid bodies, while the billet was treated as an elastic–plastic material.

The material used was the E110 alloy (Zr–1%Nb), which is employed in the fabrication of reactor core components. Since it is not included in the standard Deform material database, a custom material dataset was created based on plastometric tests. The experiments were conducted using the uniaxial compression method on cylindrical samples with a diameter of 10 mm, performed on a Gleeble 3800 system equipped with the Pocket Jaw module. The strain rate range was 0.5–15 s^{-1}, and the temperature range was 20–650 °C, corresponding to the actual conditions of the radial-shear rolling process.

Temperature control was carried out using chromel–copel thermocouples welded directly to the sample. To reduce friction, graphite foils and ceramic lubricants were applied. As a result, true stress–strain curves were obtained (Figure 3), showing a decrease in flow stress by approximately 77% when the temperature increased from 20 to 650 °C. At the same time, increasing the strain rate led to higher flow stress: this effect was minor at low temperatures but reached about 25% at 650 °C.

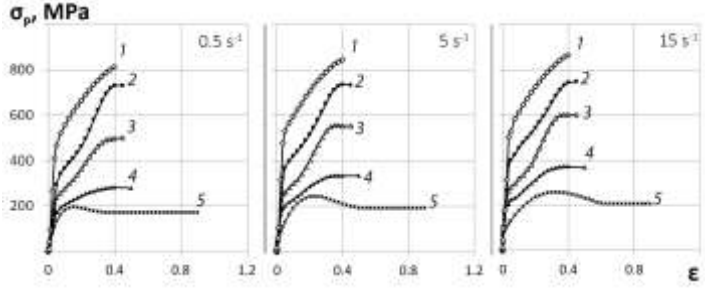

Figure 3 - Flow curves for the E110 alloy obtained using the Gleeble 3800 plastometer at strain rates ranging from 0.5 to 15 s□ ¹ and at the following temperatures: 1 – 20 °C; 2 – 200 °C; 3 – 350 °C; 4 – 500 °C; 5 – 650 °C.

Analysis of the curves showed that in the temperature range of 350–500 °C, a decrease in the strain-hardening coefficient occurs due to the activation of additional slip systems and dynamic recovery processes. At 650 °C, the curves acquire a bell-shaped form: after reaching a maximum flow stress at a strain of 0.15–0.30, a steady-state flow stage is established—typical for alloys with a hexagonal crystal structure.

Based on the obtained data, a new material database for Deform-3D was created, covering a temperature range of 20–650 °C and strain rates of 0.5–15 s^{-1}. This enabled accurate reproduction of the rheological behavior of the E110 alloy during the simulation of the radial-shear rolling process and allowed its subsequent use in further numerical experiments.

2.2 Development of a computer-based model of the radial-shear rolling process and analysis of the stress-strain state for ultrafine-grained structure formation in zirconium.

To construct an accurate model of the radial-shear rolling process in Deform, a high-precision 3D geometry of the SVP-08 mill rolls was created. The rolls were arranged symmetrically around the billet axis at an angle of 120°, ensuring uniform compression. A Cartesian coordinate system was used to define the absolute values of the reduction by calculating the displacement components of the rolls. For example, with a total reduction of 3 mm, the radial displacement of each roll was 1.5 mm, which provided accurate roll movement coordinates for the simulation.

When analyzing the stress–strain state, three key criteria were considered: equivalent strain, equivalent stress, and mean hydrostatic pressure.

Strain-Effective The simulation results revealed a helical pattern of strain accumulation, with maximum values forming along a spiral line in the roll–contact zones. In the cross-section, the distribution was highly nonuniform: the strain level reached 2.1 at the surface and decreased to zero toward the center. The radial distribution curve showed an exponential decrease in strain magnitude, indicating the formation of a pronounced structural gradient within the billet.

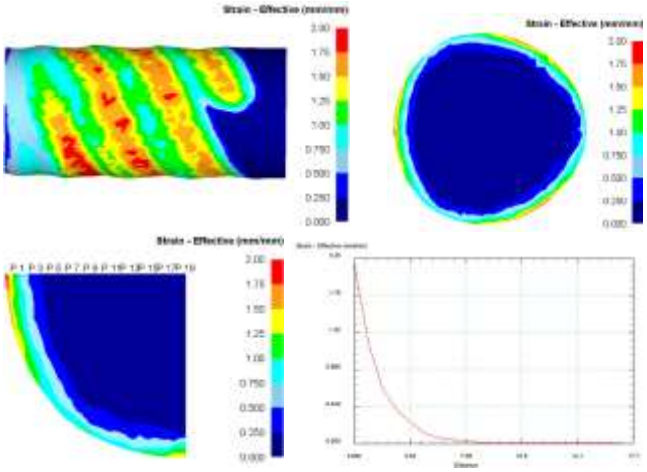

Figure 4 - Distribution of the Strain-Effective parameter in the billet.

Stress-Effective. The stress state encompassed the entire annular region of the deformation zone. Maximum values were recorded in the roll–contact areas, with the distribution exhibiting a zigzag pattern caused by variations in the roll surface taper. In the cross-section, the stresses extended throughout the entire billet volume, ranging from 313 MPa at the surface to 163 MPa at the center. The resulting curve

had a smooth parabolic shape, indicating a relatively uniform decrease in stress levels across the radius.

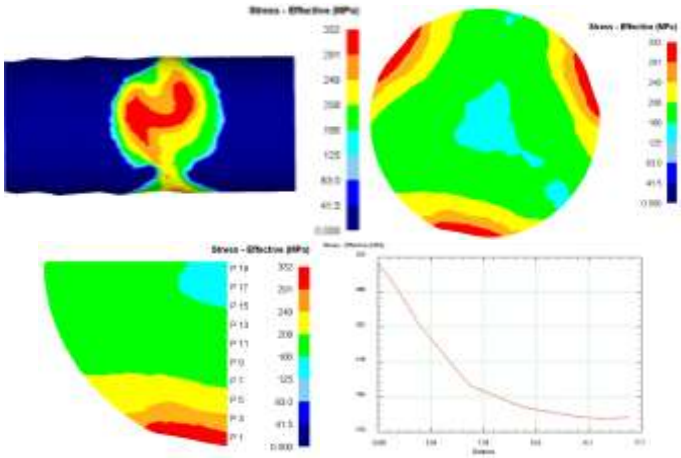

Figure 5 - Distribution of the Stress-Effective parameter in the billet.

Stress-Mean. The parameter was distributed more uniformly, forming oval-shaped zones in the contact regions. In the cross-section, a distinct alternating pattern was observed: compressive stresses at the surface (up to –558 MPa) gradually transitioned into tensile stresses in the central zone (up to +90 MPa).

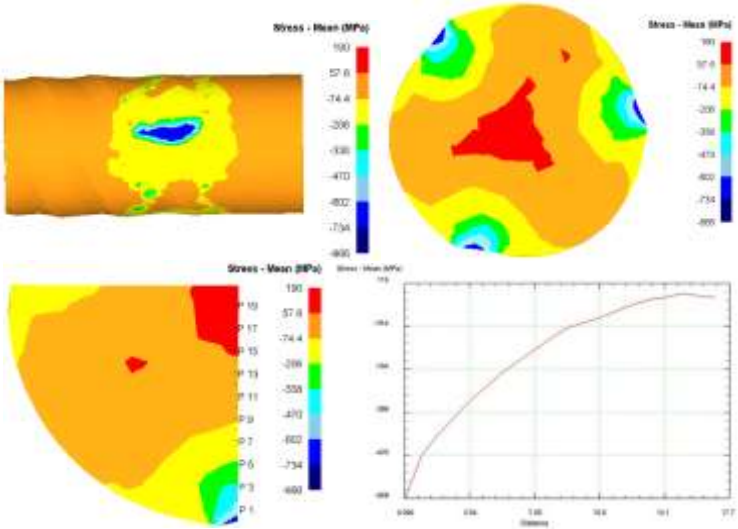

Figure 6 - Distribution of the Stress-Mean parameter in the billet.

The ratio between these stresses indicates the dominance of compressive stresses, whose magnitude exceeds that of the tensile stresses by more than sixfold. The radial-shear rolling model demonstrated an accurate reproduction of the real process. The observed distribution patterns of strain and stress are consistent with known experimental data.

The presence of high compressive stresses, combined with a pronounced deformation gradient, suggests the potential for effective grain refinement and the formation of an ultrafine-grained structure. At the same time, the gradient nature of the structural distribution across the billet cross-section highlights the possibility of targeted property control in zirconium alloys used for nuclear reactor core components.

2.3 Determination of optimal technological parameters for radial-shear rolling of zirconium using on computer-based modeling

In this study, the radial-shear rolling process of the Zr–1%Nb zirconium alloy was optimized. The deformation force level was selected as the optimization criterion, as this parameter integrally reflects the combined influence of both geometric and technological factors.

To evaluate the efficiency of the process, two rolling regimes were considered:

– **Regime 1** — with high single-pass reductions applied during the initial rolling passes;

– **Regime 2** — with small reductions at the initial stages of rolling.

Table 1 - Different Regimes of Radial-Shear Rolling.

	Regime 1			Regime 2		
Pass number	D_0, mm	D_1, mm	Reduction, mm	D_0, mm	D_1, mm	Reduction, mm
1	37	34	3	37	35.5	1,5
2	34	31	3	35.5	34	1,5
3	31	30	1	34	32	2
4				32	30	2

The simulation results showed that the maximum strain levels for both variants were comparable (22.5 and 22.8, respectively); however, the strain distribution across the cross-section differed significantly. In Regime 1, pronounced nonuniformity and local strain concentrations were observed, leading to process instability. In contrast, Regime 2 provided a more uniform strain field and a noticeable reduction in peak loads.

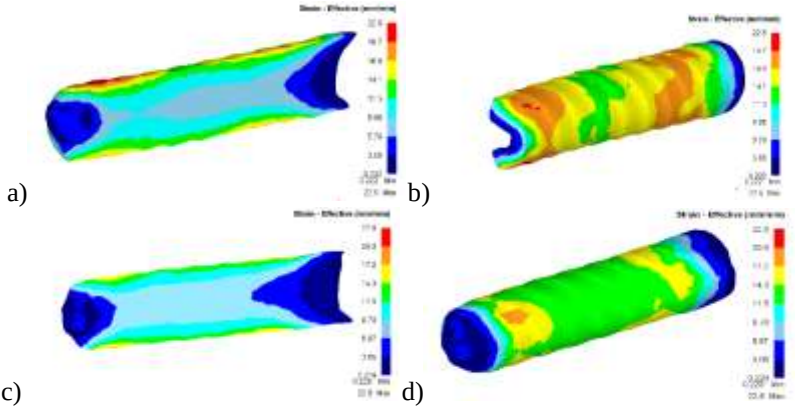

a, b – Axial and surface zones for regime 1;
c, d – Axial and surface zones for regime 2;
Figure 7 – Strain Distribution after Radial-Shear Rolling.

Variation of the billet temperature showed that lowering the heating temperature relative to the baseline (530 °C) sharply increases the deformation force. Even a 100 °C decrease leads to a load rise nearly to the limiting level. This effect is associated with increased deformation resistance and a higher risk of process instability. Conversely, exceeding the baseline temperature promotes recrystallization, which prevents the formation of an ultrafine-grained structure. Therefore, maintaining the baseline temperature with minimal deviations is the optimal solution.

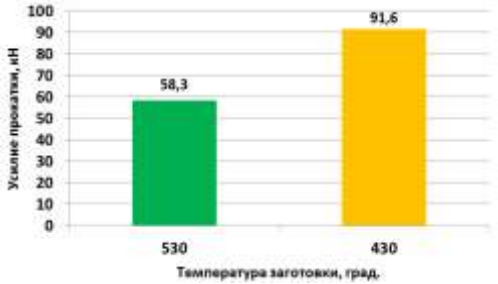

Figure 8 - Rolling Force at Different Billet Heating Temperatures.

The rolling speed proved to be a less critical parameter. Variations of ±20% from the nominal value (100 rpm) resulted in only minor fluctuations in the rolling force, within the range of 4–5%.

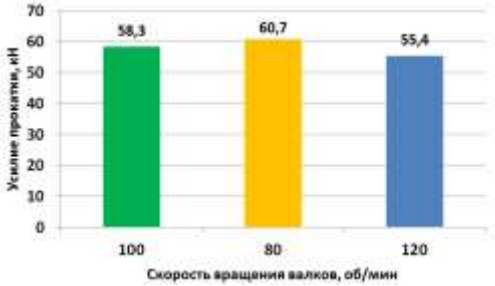

Figure 9 - Rolling force at different roll rotation speeds.

During rolling along the route 37 mm → 20 mm (eight passes, with a total strain of approximately 70%), a pronounced strain gradient across the billet cross-section was observed.

In the axial zone (0–35% of the radius), the strain level reached approximately 9.5.

In the peripheral zone (35–80% of the radius), it ranged from 19.5 to 21.5.

In the surface layers (80–100%), the strain increased up to 29–30.

Thus, the surface undergoes the most intensive deformation, promoting significant structural refinement and the formation of an ultrafine-grained (UFG) state. At the same time, the central region experiences a lower deformation level, resulting in the development of a gradient structure across the billet cross-section.

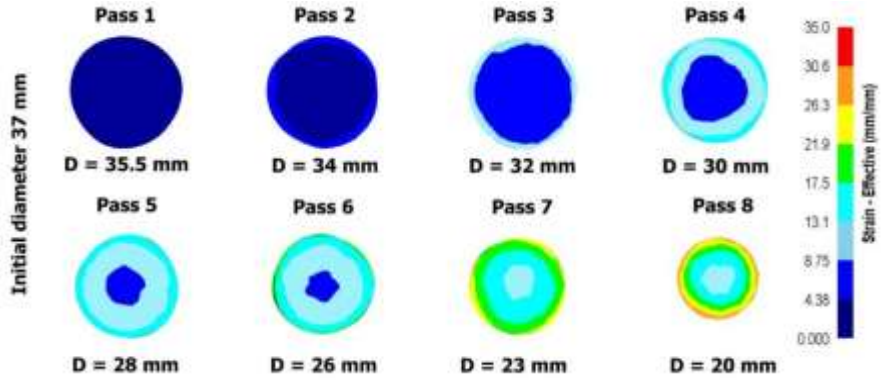

Figure 10 –Strain-Effective after sequential radial-shear rolling of a rod from 37 mm down to 20 mm in diameter.

Such a distribution pattern of deformation can be clearly explained using the vector field of metal flow directions (Figure 11). From the longitudinal section of the billet, it is evident that in the surface layers, the metal flow during radial-shear rolling exhibits a vortex-like behavior, which promotes microstructural

modification, the formation of an equiaxed morphology, and the fragmentation of grains down to the ultrafine-grained (UFG) scale.

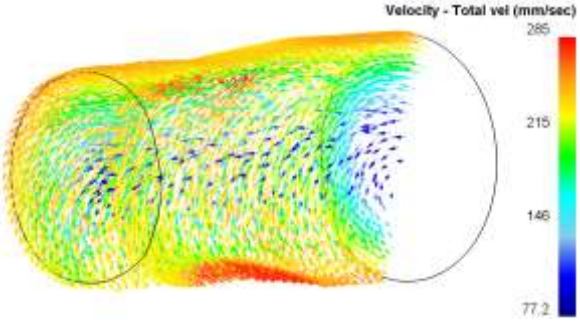

Figure 11 - Character of metal flow during radial-shear rolling.

The optimization results showed that:

– The most rational strategy is to use small reductions in the initial passes.

– Lowering the billet temperature below 530 °C is unacceptable due to the sharp increase in deformation force, while raising it leads to recrystallization.

– The rolling speed has a secondary effect, allowing variations around the nominal value.

– A characteristic gradient structure is formed, with maximum refinement at the surface and softer deformation conditions in the center.

– In all cases, the deformation force remains below the technological limit, confirming the stability and reliability of the process.

2.4 Computer-based modeling and experimental study of ECAP technology as a reference method

As a reference severe plastic deformation (SPD) method for comparison with radial-shear rolling (RSR), the Equal-Channel Angular Pressing (ECAP) technique was selected. Its use made it possible to compare the efficiency of ultrafine-grained (UFG) structure formation and the degree of refinement of the as-cast structure of the E110 zirconium alloy. Unlike RSR, ECAP provides uniform shear deformation throughout the entire cross-section, which promotes the elimination of bulk defects and improves the homogeneity of the material.

Simulation of the ECAP process with different channel intersection angles (45°, 90°, and 135°) showed that reducing the angle increases the deformation intensity and accelerates the closure of through defects. For further verification, a die with a 135° angle was selected as the least favorable case. Even under these conditions, the defect was successfully closed, confirming the high efficiency of the method.

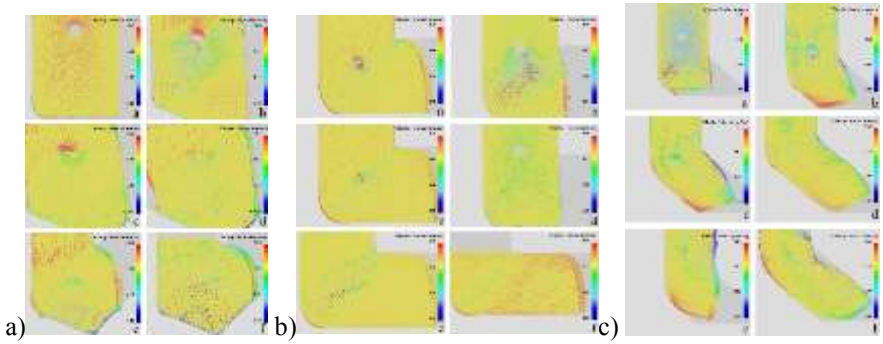

Figure 12 - Stages of through-defect closure in the model with die channel intersection angles – a) 45° b) 90° c) 135°

The distribution of strain and stress revealed that after several ECAP passes, a zone of intense deformation forms, encompassing the entire billet cross-section. The central region experiences a significantly higher degree of refinement compared to radial-shear rolling (RSR). It was established that during deformation, a predominantly compressive stress state develops, which facilitates the elimination of casting defects.

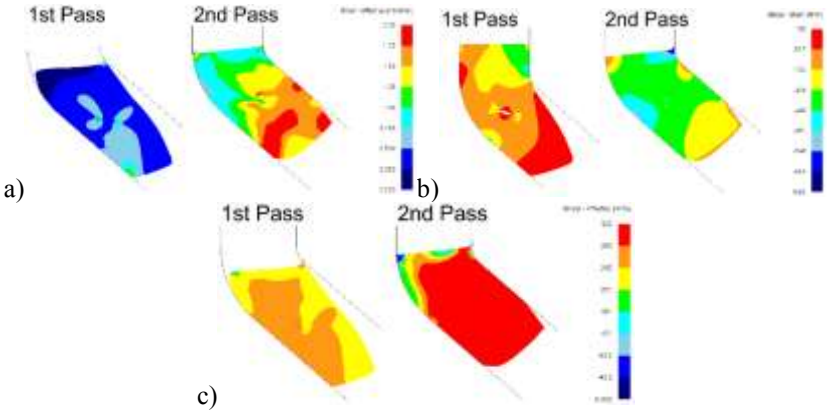

Figure 13 Distribution in the longitudinal section of the workstation: a) Strain - Effective ; b) Stress - Mean; c) Stress - Effective.

At this stage, the effectiveness of ECAP was confirmed as a method for the initial processing of small zirconium ingots, aimed at eliminating defects and producing an ultrafine-grained (UFG) structure. However, its application is limited by the size of the billets and the requirement for multiple passes, which makes this method a complementary process rather than a substitute for radial-shear rolling in industrial-scale processing.

3 Study of the structure and properties of ultrafine-grained zirconium produced by severe plastic deformation methods

3.1 Preliminary Experimental Radial-Shear Rolling of the E110 Alloy

The experimental radial-shear rolling was carried out using an industrial E110 alloy in the form of rods with a 35 mm diameter, produced by preliminary hot extrusion at 650 °C. The initial material exhibited a tensile strength of 470 MPa, a yield strength of 348 MPa, and an elongation of 34%. Rolling on the SVP-08 mill was performed at a heating temperature of 530 °C, monitored by an infrared thermal imaging camera. The process was conducted under near-limit conditions with incremental reductions of 1.5–3 mm until the minimum technological diameter of 20 mm was achieved. During deformation, a localized temperature increase of up to 150 °C was recorded, indicating the occurrence of intense shear processes within the deformation zone.

For microstructural studies, the rolled rod was sectioned into segments from which samples were prepared for transmission electron microscopy (TEM). Investigations using a JEM-1400Plus TEM revealed the formation of equiaxed, dislocation-rich grains in the peripheral zone, with sizes ranging from 500 to 1000 nm and no pronounced texture, corresponding to an ultrafine-grained (UFG) state. In the central zone, a mixture of elongated, heavily deformed grains (approximately 100 nm in width and up to 10 μm in length) and individual large grains comparable to the initial microstructure was observed. Electron diffraction patterns confirmed the presence of a preferred orientation associated with the rolling direction

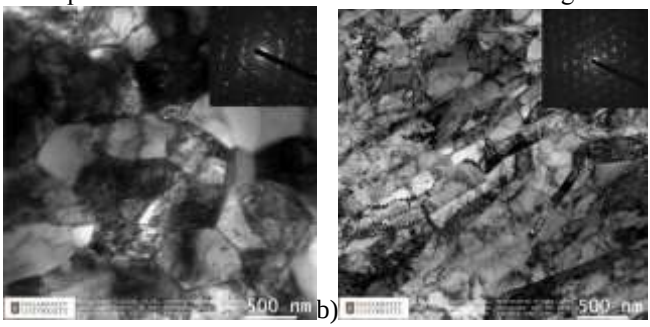

b)

Figure 14 - Microstructure of the Zr–1%Nb alloy after Radial-Shear Rolling (×15,000): a – periphery of the rod, b – Center of the rod.

The obtained results confirmed the fundamental feasibility of forming an ultrafine-grained (UFG) structure in the E110 alloy using the radial-shear rolling method. The experiment also made it possible to refine the practical aspects of performing deformation under near-limit conditions and of sample preparation for subsequent comprehensive microstructural analysis.

3.2 RSR Rolling of rods for structural evolution analysis

The next stage of the study—focused on identifying different structural types—required determining the thickness and uniformity of the UFG zone, as well as analyzing the structural and textural gradients across the cross-section.

To address this objective, a series of rolling experiments was carried out on five rods of different diameters (30, 25, and 20 mm, as well as additional reductions to 15 and 13 mm). This made it possible to obtain material for studying the intermediate stages of UFG structure formation. Unlike the previous experiment, the focus was not only on demonstrating the feasibility of the process, but also on tracking the evolution of the UFG layer and its characteristics.

A sample preparation methodology was developed, including precision sectioning of specimens, electrolytic polishing with electrolyte cooling, and optimization of etching parameters to ensure accurate microstructural observation.

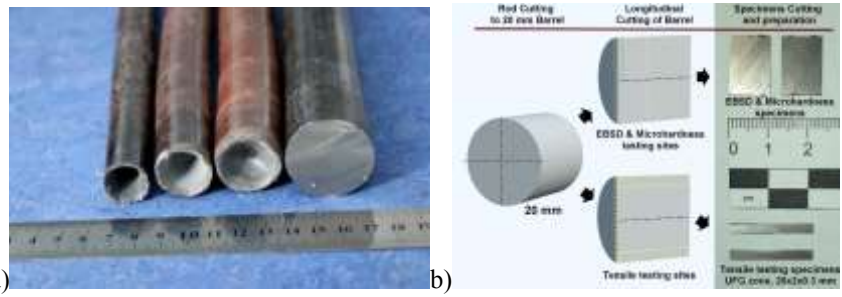

a) b)

Figure 15 – a) Rolled rods of the Zr–1%nb alloy; b) Scheme of sample sectioning for various types of analysis

The extended experimental series and the combined analytical approach made it possible to move beyond the initial confirmation of UFG structure formation toward a comprehensive investigation of its development, boundaries, and stability.

3.3 Detailed EBSD mapping of samples

To quantitatively evaluate the evolution of the grain structure after radial-shear rolling, the EBSD (Electron Backscatter Diffraction) method was employed. Maps were acquired along the rod radius with a 0.5 mm step, at a magnification of ×8000, a scanning step of 20 nm, and a mapping area of 50×50 μm. Each map contained 60 to 100 grains, ensuring statistical reliability of the results. In total, more than 100 EBSD maps were obtained and processed using HKL Tango software. The average grain area was chosen as the primary microstructural parameter, and radial distributions of this characteristic were constructed for detailed analysis of the structural gradient.

The analysis showed that in the initial sample, the average grain diameter was approximately 4 μm. After the first rolling stage (down to 30 mm), the grain size decreased to 1.0–1.2 μm in the central region and to about 0.7 μm in the peripheral zone.

At all subsequent stages (25–13 mm), grain refinement initiated in the surface regions and gradually propagated inward, forming a stable ultrafine-grained (UFG) layer approximately 2 mm thick, with a grain diameter of 0.6–0.7 μm. In the central regions, the refinement proceeded more slowly, reaching submicron dimensions only after substantial total reductions.

In addition, a gradient was observed both in grain size and in grain shape. The grain diameter decreases toward the surface, while the aspect ratio increases, then drops sharply at a depth of 1–1.5 mm. IPF maps revealed changes in grain orientations with decreasing rod diameter, indicating the formation of a distinct textural gradient. The EBSD maps and distribution plots of the average grain diameter and aspect ratio across the cross-sections of the 15 mm and 13 mm billets are presented in the figure 16.

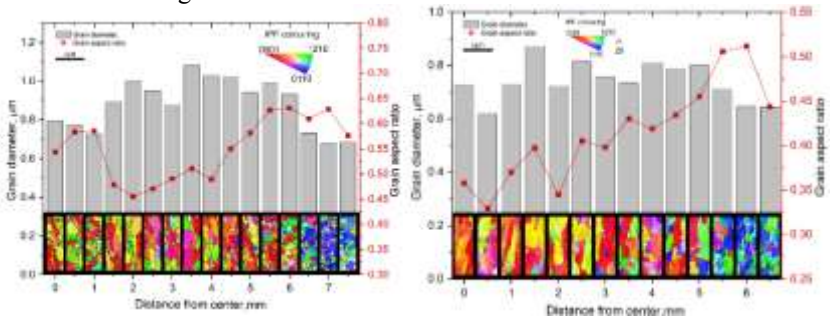

Figure 16 – EBSD Maps and Distribution Plots of Average Grain Diameter and Aspect Ratio across the Cross-Sections of Billets: a) 15 mm; b) 13 mm.

3.4 Analysis of texture evolution during the rolling process.

The texture analysis of the zirconium rods after radial-shear rolling was carried out using Kearns parameters, calculated from the EBSD data. In the initial annealed sample, a weak residual texture was observed: the f-parameter in the axial direction averaged 0.260, which is lower than in the normal (0.379) and transverse (0.361) directions.

After rolling down to 30 mm, a distinct textural component characteristic of zirconium emerged: the f-parameters in the transverse and normal directions reached 0.500–0.540, while in the rolling direction, the average value was 0.046. In the surface zone, a local increase up to 0.112 was recorded.

With a further reduction in diameter to 25 mm and 20 mm, an increase in the f-parameter in the rolling direction was observed in the surface layers (up to 0.171 and 0.195, respectively), although the average values remained low (0.041 and 0.039). The most pronounced changes were found in the 15 mm sample, where at a depth of 1 mm, the f-parameter reached 0.805, gradually decreasing to 0.406 at the surface. After rolling down to 13 mm, the parameter values decreased, and the distribution became less uniform. The pole figures and Kearns parameter distributions for the 13 mm and 15 mm samples are shown in Figure 17.

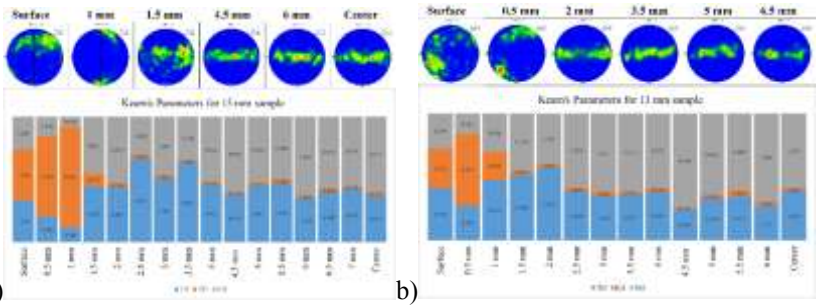

a) b)

Figure 17 – Pole Figures and Kearns parameter distribution for samples: a) 15 mm; b) 13 mm.

Thus, as the diameter decreases from 35 mm to 15 mm, there is a noticeable strengthening of the texture in the rolling direction, associated with the development of intense shear deformation. With further reduction to 13 mm, a partial weakening and instability of the texture are observed, which may indicate saturation or a change in the deformation mechanism. The thickness of the surface layer with elevated f-parameter values decreases from approximately 2.5 mm (at 30 mm diameter) to 1 mm (at 13 mm). The obtained results are consistent with the vortex-like metal flow pattern revealed by FEM simulation.

3.5 TEM analysis of the fine structure in rolled zirconium samples.

For a detailed analysis of microstructural defects in characteristic regions of the rod, investigations were carried out using transmission electron microscopy (TEM). Areas with different structural states were selected: peripheral zones exhibiting an ultrafine-grained (UFG) structure and central zones characterized by a pronounced rolling texture. The analyzed specimens were taken from rods rolled down to 15 mm and 20 mm in diameter.

The investigations revealed that the structure of the central region is in a state of active transformation under the influence of high deformation and vortex-like metal flow. In this area, the fragmentation and rotation of elongated textured grains were observed, along with occasional cases of grain coarsening and merging, associated with elements of dynamic recrystallization. A distinctive feature of this process is its cluster-type rearrangement: regions of grains with similar orientations are formed, separated from neighboring clusters by high-angle misorientation boundaries.

In the peripheral regions, the structure is stable and typical of an ultrafine-grained (UFG) state: submicron grains saturated with dislocations are observed, featuring a well-developed network of intergranular dislocations.

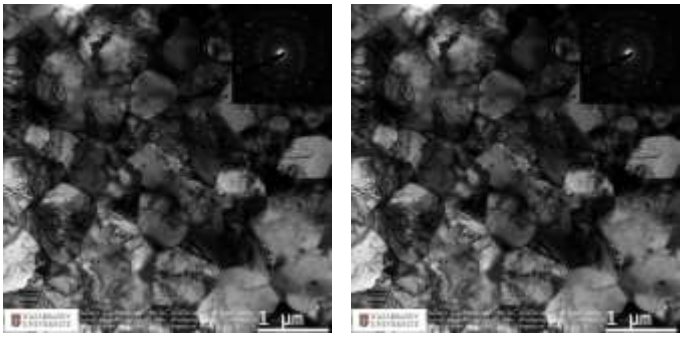

Figure 18 – TEM images of the surface zone of the rod.

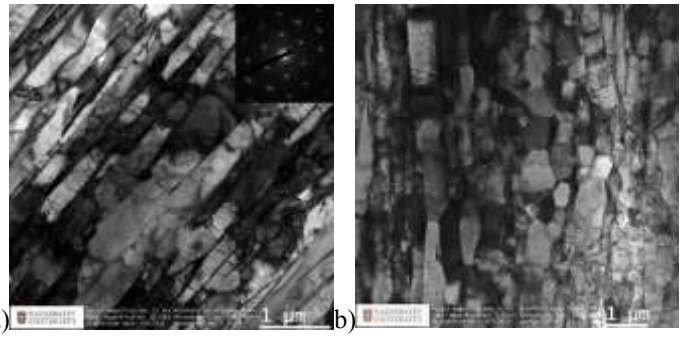

a) b)
Figure 19 – TEM images: a) Axial zone; b) Transition zone of the rod.

These findings are in good agreement with previously reported results for ultrafine-grained (UFG) materials produced by more energy-intensive methods.

3.6 Study of mechanical properties of rolled zirconium samples.

To evaluate the mechanical properties of the rolled samples, Vickers microhardness measurements were performed with a 0.5 mm step along the rod radius, and tensile tests were carried out in three characteristic zones — the peripheral, central, and intermediate (½ radius) regions.

The microhardness profiles revealed differences between the rods with diameters of 20 mm and 15 mm. In both cases, the values ranged from HV 150 to 190, with higher hardness recorded in the central region compared to the surface layers (a difference of 30–40 units). For the Ø15 mm rod, the decrease in microhardness toward the periphery was more pronounced. This distribution pattern is attributed to dynamic softening and possible polygonization or recrystallization processes in the near-surface layers, caused by the combination of the rolling temperature (~500 °C) and deformation-induced heating (up to 200 °C).

Tensile tests were carried out on the Ø15 mm sample using thin longitudinal strips, which made it possible to evaluate the mechanical properties of individual

zones. The peripheral regions exhibited slightly lower values of yield strength, ultimate tensile strength, and elongation, which is attributed to defect accumulation and dynamic softening. Nevertheless, the ultimate tensile strength in this zone reached approximately 540 MPa, significantly exceeding both the initial material properties and the requirements for nuclear fuel cladding materials. Samples from the central and intermediate zones demonstrated similar stress–strain curves, with a slight increase in strength observed in the central region. Tensile test curves by zone for the 15 mm diameter sample are presented in Figure 20, and the detailed tensile graphs by zone for the same sample are shown in Figure 21.

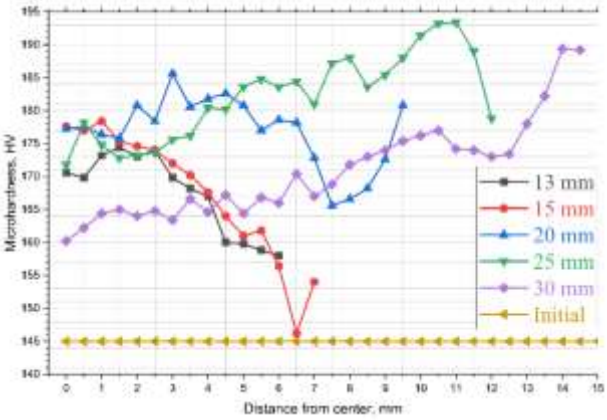

Figure 20 – Microhardness profiles across the cross-sections of all rolled samples.

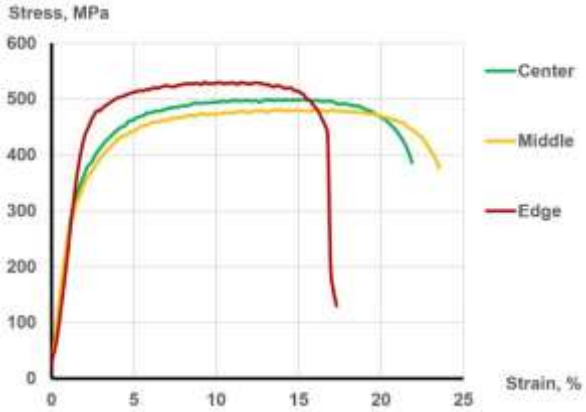

Figure 21 - Tensile test curves for different zones of the sample rolled down to a diameter of 15 mm.

3.7 Experimental processing of E110 billets by ECAP as a reference method

For experimental verification of the model, the configuration with a die channel intersection angle of 135° was selected, as it presents the greatest challenge for defect closure. A die with a 30 × 24 mm channel, made of tool steel, was prepared with polished walls and graphite lubrication to reduce friction. The billets were heated to 530 °C, and the die was preheated to approximately 200 °C, which helped minimize temperature gradients and prevent defect formation. The pressing operation was performed on a hydraulic press with a maximum load capacity of 1500 kN and a ram speed of 5–10 mm/s.

The experiment involved two passes, with the billet rotated by 180° between cycles to ensure uniform strain distribution. However, during the second pass, several technological difficulties arose. Due to partial temperature loss in the billet, the deformation resistance increased, which led to a rise in the applied load and a reduction in the stiffness of the die's working section. As a result, jamming of the billet and punch was observed, limiting the number of successful passes to a maximum of two.

3.8 Study of the structure and properties of zirconium processed by ECAP.

Metallographic and EBSD analysis showed that after the first ECAP pass, the structure of the E110 alloy retained a relatively coarse grain size (average ≈ 2.6 μm, with some grains up to 15 μm), but noticeable shape changes were already observed, indicating the onset of grain refinement processes. After the second pass, significant refinement occurred: the average equivalent grain diameter decreased to approximately 1.7 μm, with a range of 0.5–11 μm.

However, a high degree of grain size heterogeneity remained, and IPF maps revealed the initial formation of crystallographic texture. The EBSD structural maps and pole figures for the first and second ECAP passes are shown in Figures 22 and 23, respectively.

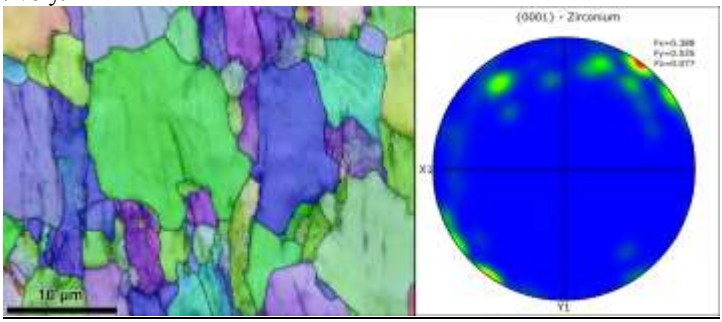

Figure 22 - EBSD map of zirconium after the first ECAP pass.

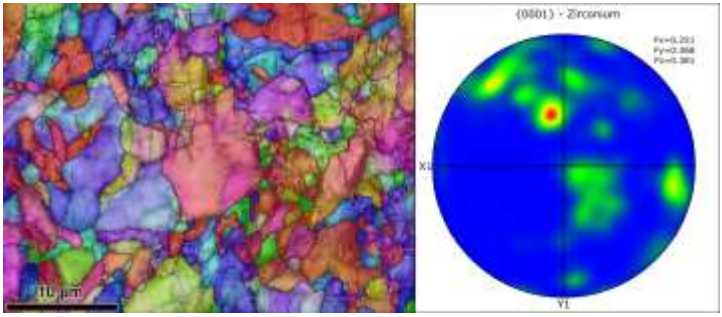

Figure 23 - EBSD map of zirconium after the second ECAP pass.

Microhardness measurements showed an increase in this parameter from 145 HV (initial state) to 158.9 HV after the first pass and 171.5 HV after the second pass. The observed hardening is attributed to dislocation accumulation, grain refinement, and localized dynamic recrystallization processes.

4 Study of the applicability of severe plastic deformation methods for processing zirconium ingots.

4.1 Study of the Processing of Cast Zirconium Structure by Radial-Shear Rolling (RSR)

At this stage, the possibility of applying radial-shear rolling (RSR) for processing remelted ingots made of E110 zirconium alloy (Zr–1%Nb) is considered. The main focus is on assessing the efficiency of this method as a tool for eliminating casting defects, transforming the brittle cast structure into a ductile one, and subsequently forming an ultrafine-grained (UFG) state in the material. For this study, an ingot produced in a vacuum induction furnace was used (Figure 24).

Chemical analysis confirmed that the composition of the starting material corresponded to the nominal E110 alloy, ensuring the validity of subsequent experiments.

Rolling was carried out on the RSR-10/30 mill in two stages. During the first stage, at a temperature of 800 °C and with large single reductions, intensive densification of the structure and closure of casting defects occurred. The second stage, conducted at 530 °C with small deformation increments, resulted in significant grain refinement, corresponding to the conditions required for obtaining an ultrafine-grained (UFG) structure, as previously reported in the literature. Temperature control during rolling was performed using a real-time infrared thermographic system, ensuring precise reproduction of the specified processing parameters.

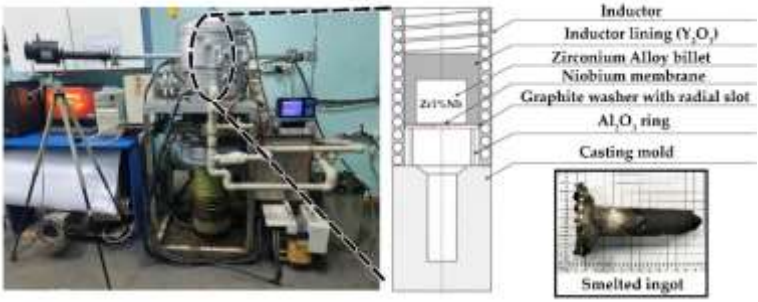

Figure 24 - Scheme of the vacuum induction melting furnace.

Figure 25 - Billets after each stage of radial-shear rolling.

4.2 Study of the structure and casting defects of the ingot after RSP.

The structural analysis of the cast samples after rolling was performed according to the same protocols as in the previous rolling experiment.

During the first stage, conducted at a temperature of 800 °C with a diameter reduction from 30 to 20 mm, a pronounced grain refinement was observed on the rod surface. According to EBSD analysis, the peripheral regions exhibited intense structural transformation and the formation of fine grains, while the central region retained features of the as-cast or transitional structure, indicating a lower deformation intensity. Phase analysis confirmed the predominance of the α-phase of zirconium, while residual β-phase regions were detected near the surface. The crystallographic texture displayed strong anisotropy in the peripheral zone and weak orientation in the central area.

The second processing stage was carried out at a temperature of 530 °C, with a successive reduction of the rod diameter to 13 mm. Microstructural analysis revealed that in the surface layers, the grains reached submicron sizes as a result of intense plastic deformation and dynamic recrystallization processes. In the central region, elongated grains aligned along the rolling direction were still observed; however, even there, the structure was significantly refined compared to the initial state. The phase composition was characterized by an almost complete transformation into the α-phase, due to the instability of the β-phase under the

selected temperature conditions. Texture analysis showed pronounced anisotropy in the surface region and weaker orientation in the central zone, confirming the reorientation of grains under the influence of deformation.

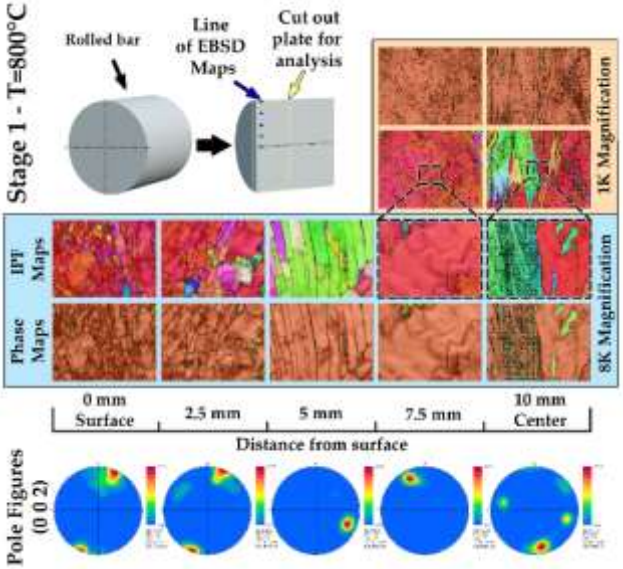

Figure 26 – EBSD Analysis of the First Stage of Zirconium Ingot Processing by Radial-Shear Rolling down to 20 mm.

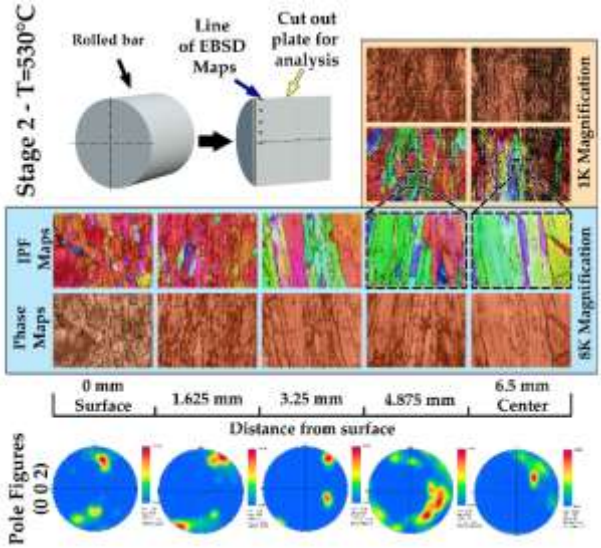

Figure 27 – EBSD Analysis of the Second Stage of Zirconium Ingot Processing by Radial-Shear Rolling down to 13 mm.

Special attention was given to the analysis of the shrinkage cavity that was initially present in the cast ingot. After rolling, it remained as a residual internal defect of star-shaped morphology with radial cracks. Despite the overall reduction in its size, proportional to the reduction ratio, complete closure of the defect was not achieved. This indicates that the plastic deformation intensity under the selected processing conditions was insufficient to fully eliminate the shrinkage cavity (Fig. 28).

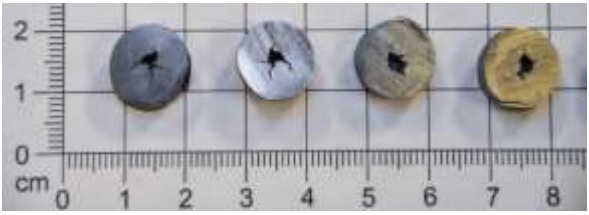

Figure 28 – Segments of the rolled ingot with the remaining shrinkage cavity.

Thus, the results demonstrate that radial-shear rolling provides intense grain refinement and phase stabilization of the zirconium α-phase, yet it does not ensure complete elimination of large casting defects. This limitation should be taken into account when considering the practical implementation of the method.

4.3 Study of casting defect closure using ECAP methods.

An experimental verification of the potential of ECAP (Equal Channel Angular Pressing) for closing casting defects in zirconium alloys was carried out. Since obtaining a sufficient amount of as-cast material with natural defects was not feasible, the defect was simulated by drilling a 5 mm diameter hole in billets made of the zirconium alloy. The chosen defect size was based on data from previous studies conducted on forging and radial-shear rolling processes.

After the first pass through the die, the defect underwent only a partial shape modification: it became compressed vertically and elongated along the deformation direction, but the edges of the cavity did not fully merge, indicating insufficient accumulated deformation intensity. The second pass, performed with a 180° rotation of the billet, resulted in almost complete closure of the macrodefect, which became invisible to the naked eye. However, detailed analysis revealed a residual crack with a width of 10–25 μm, extending along the former cavity. The defect significantly decreased in size due to the higher deformation degree and partial welding of the metal edges, but it was not completely eliminated. The appearance of the initial sample and the defect closure process during pressing are shown in Figure 29.

The presence of a residual defect can be attributed both to the limited processing temperatures of the ECAP method and to possible surface oxidation within the cavity area, which hinders complete metal bonding. To achieve full elimination of such defects, additional measures may be required—such as post-deformation heat treatment or optimization of deformation parameters, including an increased number of passes or a reduction of the die channel intersection angle.

Based on the results of the experiment, it can be concluded that the ECAP method is effective in reducing the size of large casting defects in zirconium alloys. Although a residual crack remained, the obtained results demonstrate the promising potential of this method for the practical processing of cast billets and the subsequent improvement of their operational properties.

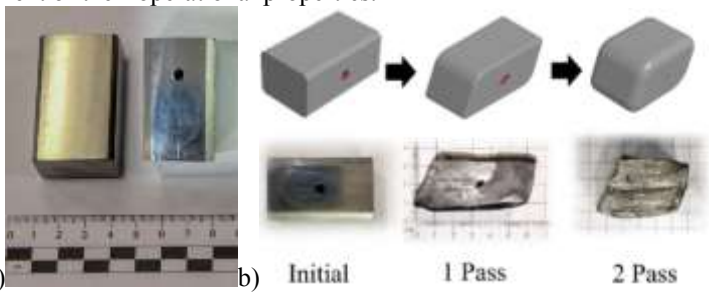

Figure 29 – Appearance of the initial sample (a) and the defect closure process during pressing (b).

5 Study of the effect of temperature on the stability of the structure and mechanical properties of zirconium crystals.

5.1 Investigation of the effect of annealing at various temperatures on the obtained structure and properties

Investigating the effect of temperature on the structure and mechanical properties is crucial, since a nuclear reactor operates under high temperatures and pressures. Accordingly, to characterize the behavior of UFG zirconium, tests were planned at three elevated-temperature points.

For the experiment, three characteristic temperature points were selected: the operating temperature of most reactors (380 °C), the recrystallization temperature of the E110 alloy (580 °C), and the accident temperature corresponding to the LOCA scenario (1000 °C). Annealing of longitudinal-section plates, cut from the final 15 mm-diameter rod containing the most developed ultrafine-grained (UFG) zone, was carried out in a high-purity argon atmosphere. Subsequent EBSD analysis was performed along the radial cross-section, allowing for a detailed assessment of the microstructural evolution at each temperature condition.

The results showed that at 380 °C, after a two-hour exposure, the structure remained virtually unchanged, indicating the stability of the UFG state under the typical operating conditions of a reactor. At 580 °C, a rapid development of recrystallization processes was observed: within 30 minutes, the grain size increased by a factor of 2–3, and large equiaxed grains appeared in the central regions. With further holding time, the structure became uniformly coarse-grained, reaching a stable annealed state after 90–120 minutes. Annealing at 1000 °C for 2 hours led to complete recrystallization and the formation of a typical Widmanstätten structure.

Microhardness testing confirmed the observed microstructural changes. For samples annealed at 380 °C, only a slight decrease in hardness was recorded, without

alteration of the distribution profile—this behavior is attributed to the relaxation of internal stresses. At 580 °C, a significant drop in microhardness was observed, accompanied by a flattening of the hardness profile across the entire cross-section. This effect became especially pronounced after holding times exceeding 60 minutes, when differences between the hardness curves became minimal. At 1000 °C, the microhardness was even lower than after prolonged annealing at 580 °C, which is explained by the completion of recrystallization and the further coarsening of the grain structure.

Thus, the conducted study demonstrated the high stability of the ultrafine-grained (UFG) structure at typical reactor operating temperatures, as well as its rapid degradation under conditions corresponding to the recrystallization temperature and accident-level heating. These results are crucial for understanding the operational limits and applicability boundaries of ultrafine-grained zirconium in nuclear energy systems.

5.2 Study of the Stability of Mechanical Properties at Various Temperatures

Tensile tests at elevated temperatures were conducted on narrow strips cut from the three characteristic zones of the 15 mm diameter rod possessing an ultrafine-grained (UFG) structure. The testing procedure followed the previously established protocols, with the only modification being that the experiments were performed at 380 °C, 580 °C, and 1000 °C. Before testing, the samples were heated in a protective atmosphere, held for two hours at the target temperature, and then subjected to tensile loading directly at that temperature.

The results showed that at 380 °C, only a slight reduction in mechanical properties was observed across the entire cross-section of the material, confirming the stability of the structure under typical reactor operating conditions. At 580 °C, the mechanical properties became more uniform, with a significant decrease in ultimate tensile strength and a slight increase in elongation, indicating the onset of recrystallization and microstructural softening. Tests conducted at 1000 °C revealed an extremely low strength level and a marked increase in ductility, which are associated with complete recrystallization and grain coarsening. Tensile test curves at different temperatures for both the initial sample and the UFG zone are shown in Figures 30 and 31.

All obtained mechanical property values comply with the requirements of ASTM B-351 and generally exceed those of conventionally manufactured bars, particularly in terms of strength. However, the elongation (δ) was found to be lower than expected for a fully recrystallized state. To improve ductility, it is advisable to apply additional heat treatment to complete the recrystallization processes. According to the microhardness data, an annealing regime at 580 °C with a 90-minute holding time ensures uniformity of structure and properties across the bar cross-section, although it is accompanied by some grain coarsening.

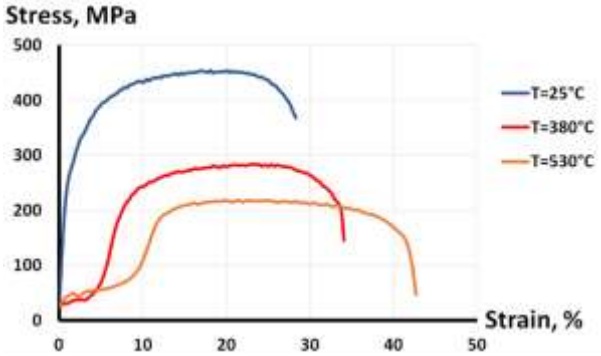

Figure 30 – Tensile test curves at different temperatures for the initial sample.

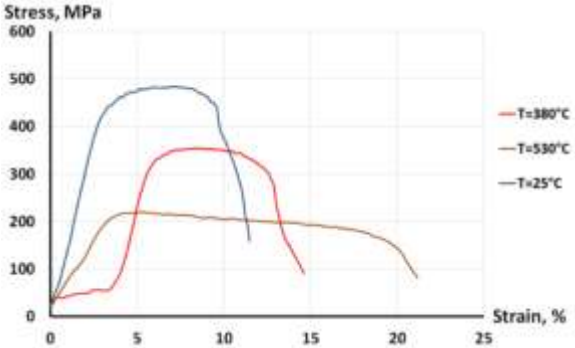

Figure 31 – Tensile test curves of the ultrafine-grained (UFG) zone obtained at different temperatures.

6 Irradiation of ultrafine-grained zirconium with heavy ions for simulating fission fragment damage and assessing material suitability for nuclear reactor applications

6.1 Testing program for the processed material using a particle accelerator

The study involved the simulation of radiation damage in ultrafine-grained zirconium alloy E110 using heavy-ion irradiation at the DC-60 accelerator complex of the Astana branch of the Institute of Nuclear Physics. Irradiation with krypton ions (□□Kr¹□□) at an energy of 17.1 keV and various fluences (5×10^{13}, 5×10^{1}□, and 5×10^{1}□ ions/cm²) made it possible to reproduce displacement cascades similar to those caused by neutron exposure, while avoiding induced radioactivity in the material. This technique enabled the accumulation of high radiation doses within a short period of time and allowed precise control over irradiation conditions.

For the experiments, samples in the form of 1 mm-thick plates were cut from bars with diameters of 15 mm (ultrafine-grained structure) and 35 mm (initial coarse-grained structure). This configuration made it possible to study the full microstructural gradient and to perform a comparative analysis of the initial and

strengthened states. Additionally, 3 mm TEM discs were prepared for fine-structure analysis, along with two sets of plates intended for EBSD mapping, nanoindentation, and microhardness measurements.

The samples were mounted on a water-cooled target holder inside the irradiation chamber of channel No. 3 of the accelerator, ensuring stable temperature conditions and uniform exposure. Beam parameter monitoring confirmed a particle flux uniformity across the sample surface within 10%, with the maximum ion incidence angle not exceeding 3°. The calculated penetration depth was approximately 13 μm, which confines the radiation-damaged region to the near-surface layer of the material.

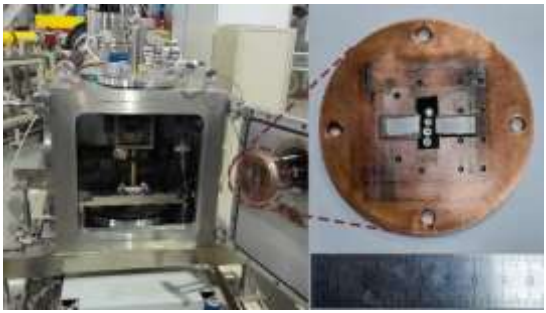

Figure 32 - Irradiation chamber of channel No. 3 and the target holder of the DC-60 accelerator with the mounted sample assembly.

The chosen approach made it possible to simulate radiation exposure under conditions where neutron experiments are constrained by long durations and strict requirements for handling radioactive specimens. Despite the limitation in damage depth, ion irradiation combined with local analysis techniques (nanoindentation, TEM, and EBSD) serves as an effective tool for investigating the microstructural stability and property evolution of structural materials intended for nuclear reactor applications.

6.2 Study of Fine Structure Evolution in Ultrafine-Grained Zirconium after Irradiation

The study presents the results of fine-structure analysis of zirconium specimens after heavy-ion irradiation. Pre-prepared and pre-mapped TEM samples were used for examination, since post-irradiation preparation of thin foils from bulk irradiated material is not feasible, and correlating local microstructural changes to specific regions becomes highly limited. This approach enabled a comparative analysis of characteristic radiation-induced modifications in both the ultrafine-grained and the initial coarse-grained structures.

The investigation revealed that at the highest fluence of 5×10^{15} ions/cm^2, both the ultrafine-grained and the initial materials exhibited severe damage in thin regions. This was manifested by the disappearance of transparent zones, changes in edge geometry, and the destruction of delicate areas. At the intermediate fluence of

5×10^{14} ions/cm^2, a pronounced reduction of transparent regions was also observed, accompanied by an increase in the thickness of the amorphized layer and a general deterioration of imaging conditions. In the initial coarse-grained specimens, partial blurring of grain boundaries due to defect accumulation was detected, whereas the ultrafine-grained material demonstrated a more stable and resistant structural state.

At the lowest irradiation level (5×10^{13} ions/cm^2), no significant structural changes were detected: the dislocation network remained largely intact, although some densification and surface amorphization were observed. In certain cases, specimens irradiated at a fluence of 5×10^{14} ions/cm^2 exhibited point defects localized near dislocations, indicating the onset of radiation-induced microstructural transformations.

The general view of the thin region suitable for TEM observation demonstrates that specimens irradiated at the maximum fluence of 5×10^{15} ions/cm^2 are unsuitable for detailed analysis, both for the initial material and the ultrafine-grained state. The entire thin area is severely damaged, which is evident not only from the complete absence of transparent regions but also from a pronounced change in edge geometry-showing flattening and detachment of protruding thin sections.

6.3 Nanoindentation-based analysis of changes in Young's Modulus.

To evaluate the effect of heavy-ion irradiation on the mechanical properties of ultrafine-grained zirconium alloy E110, nanoindentation was employed. Unlike conventional hardness testing methods, this technique is based on recording the indenter's load–displacement curve rather than measuring the residual imprint, which enables the investigation of both elastic and non-plastic materials while also allowing the determination of the Young's modulus. The method requires minimal sample preparation, provides the capability to collect large volumes of statistical data, and is particularly effective for examining surface layers only a few micrometers thick.

The tests were carried out using a TI Premier system (Bruker) equipped with a Berkovich indenter under a load of 10,000 μN. For each specimen, five regions were selected along the cross-section of the bar, each containing 25 indents. Analysis of the loading–unloading curves was performed using the Oliver–Pharr method in the TriboScan software package, which allowed determination of the reduced elastic modulus and its subsequent conversion to the Young's modulus.

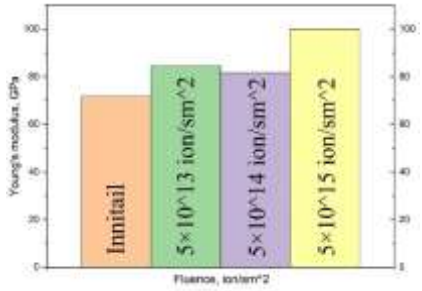

Figure 33 – The Young's modulus for the ultrafine-grained (UFG) zone before and after irradiation.

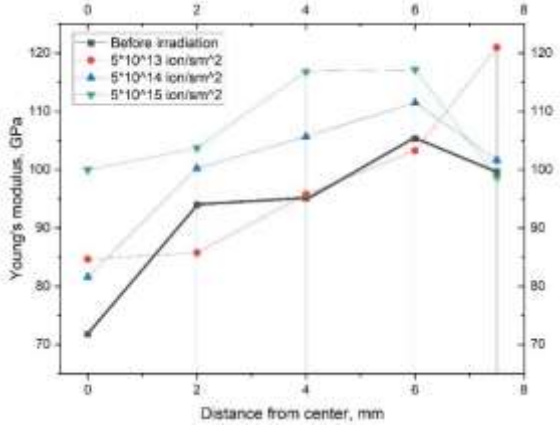

Figure 34 - The Young's modulus across the specimen cross-sections.

The results demonstrated a systematic increase in the Young's modulus with increasing irradiation fluence. A pronounced gradient was preserved across the bar cross-section: the most significant changes were observed in the central region, whereas the peripheral ultrafine-grained zone exhibited a less pronounced increase in modulus. At low irradiation doses, atypical fluctuations were detected, which can be attributed to dislocation annihilation processes under mild exposure. With further fluence increase, defect accumulation resumed, leading to a rise in the material's stiffness.

The obtained data confirm that the ultrafine-grained state of zirconium exhibits higher radiation resistance: although the Young's modulus increased uniformly across the cross-section, the UFG region showed lower sensitivity to defect accumulation compared to the initial coarse-grained structure.

6.4 Study of Changes in Vickers Microhardness (HV)

The microhardness analysis of the irradiated specimens followed the same procedure as the nanoindentation tests. Measurements were performed at five characteristic points along the radius of the specimen cross-section, with five indents made at each point, resulting in a total of 25 measurements per specimen and 100 measurements for the entire series. Microhardness was determined using the Vickers method on a Shimadzu HMV-G (Japan) tester under a load of HV 0.5 (4.903 N) with a dwell time of 5 seconds. The use of a low load made it possible to limit the indentation depth to a value comparable to the thickness of the radiation-damaged layer (≈13 μm).

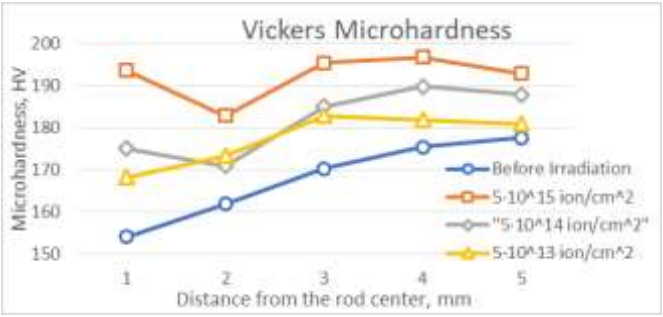

Figure 35 – Vickers microhardness (HV) across the bar cross-section.

The obtained results showed full agreement with the nanoindentation data: a pronounced property gradient across the cross-section was retained, and an increase in microhardness was observed with rising irradiation fluence. The most significant changes in properties occurred in the central part of the bar, which had undergone the least plastic deformation during material processing. In contrast, the peripheral ultrafine-grained region exhibited much weaker variations, indicating its resistance to radiation-induced hardening.

Quantitative analysis revealed that for the conventionally deformed texture, the difference in properties reached 39 HV (25%), whereas for the ultrafine-grained structure it was only 15 HV (8%). This indicates a significantly higher radiation resistance of the UFG zirconium and highlights its potential as a structural material less susceptible to radiation-induced hardening and associated degradation processes.

Conclusion

In the course of the present study, an applied scientific problem was addressed concerning the development and experimental validation of a technology for forming an ultrafine-grained (UFG) structure in zirconium alloys using severe plastic deformation methods, in particular radial-shear rolling (RSR), followed by analysis of the structural and performance characteristics of the resulting material.

The work encompasses the entire research cycle—from the justification of scientific relevance and significance, theoretical modeling of the processes, and development of technological parameters to full-scale experimental studies, comprehensive microstructural and mechanical characterization, and evaluation of the radiation resistance of the produced material.

The relevance of this work arises from the need to improve the performance characteristics of structural materials used in the core of nuclear reactors, such as zirconium alloy fuel claddings. Contemporary trends in nuclear energy development demand materials capable of withstanding extreme operating conditions, including high temperatures, intense neutron flux, aggressive chemical environments, and prolonged service lifetimes. The main limitations of conventional zirconium-based materials include irradiation-induced property degradation, radiation growth, creep, formation of brittle hydrides, corrosion, and crack propagation.

Within the framework of this study, the use of an ultrafine-grained (UFG) structure is proposed as an effective approach to improving the properties of zirconium alloys. The physical basis for the enhancement of strength and radiation resistance with decreasing grain size to the ultrafine scale is substantiated. It is established that a highly dispersed structure promotes the effective suppression of radiation-induced defects due to the increased density of grain boundaries and the activation of self-healing mechanisms associated with boundary migration and vacancy absorption.

A key element of the dissertation research was the application of the radial-shear rolling (RSR) method, which possesses a unique capability to generate large plastic deformations with pronounced shear components and vortex metal flow throughout the billet volume. This process enabled not only significant grain refinement but also the formation of a gradient structure across the specimen cross-section, combining an ultrafine-grained state in the peripheral zone with a submicrocrystalline or recrystallized structure in the central region. Such an approach made it possible to achieve enhanced mechanical properties while maintaining sufficient ductility. As part of the study, a finite element model of the RSR process was developed using the DEFORM-3D software package, allowing detailed analysis of the stress–strain state of the billet under conditions of intense deformation. The calculations identified the optimal rolling parameters, including temperature, roll rotation speed, tooling geometry, and friction coefficient. The simulation results served as the basis for designing experimental regimes and verifying the computational model.

The experimental part of the work included a series of rolling trials of zirconium billets (E110 alloy) conducted on industrial-scale RSR-10/30 and RSR-14/30 mills. The obtained samples underwent comprehensive structural and property characterization. Scanning electron microscopy (SEM/EBSD) and transmission electron microscopy (TEM) were employed to study the evolution of the microstructure, revealing grain size distribution, boundary character, presence of substructural elements, and texture features. It was established that the fraction of the ultrafine-grained (UFG) structure in the transverse cross-section of the billet may

reach up to 35–40% of the outer layer, forming a distinct gradient morphology. Crystallographic texture analysis using the EBSD method enabled the determination of grain orientations and the calculation of Kearns parameters, which characterize the degree of anisotropy of the material. It was found that the RSR process promotes the formation of a predominantly radial–basal texture, favorable in terms of resistance to radiation growth. The obtained Kearns parameters (f_R – radial, f_T – transverse, f_L – longitudinal) indicate that the resulting texture is close to the optimal one for nuclear fuel claddings.

The mechanical properties of the samples were evaluated using static tensile testing and microhardness measurements. The obtained ultimate tensile strength and microhardness values demonstrated more than a twofold increase in strength compared to the initial material, while maintaining satisfactory ductility. A clear correlation was observed between local microstructure and hardness: regions with an ultrafine-grained (UFG) structure exhibited the highest values. An important part of the research involved the simulation of radiation damage through heavy-ion irradiation conducted at the DC-60 accelerator. This methodology enables the reproduction of effects analogous to those caused by fission fragment damage in nuclear fuel. Following irradiation, a repeated analysis of the microstructure and mechanical properties was performed. It was established that the material with a UFG structure retained a stable morphology, exhibited moderate radiation-induced hardening without embrittlement, and maintained the stability of the Young's modulus. These results indicate the high potential of the developed material for long-term operation under reactor conditions.

Comparative experiments were also carried out using equal channel angular pressing (ECAP) as a reference method for obtaining an ultrafine-grained (UFG) structure. It was shown that the structure produced by the radial-shear rolling (RSR) method exhibits a comparable degree of grain refinement but features a more favorable gradient morphology and superior technological scalability.

Additionally, the potential of applying the RSR method to zirconium ingots with an as-cast structure was investigated. It was found that RSR is capable of effectively closing shrinkage and microporosity defects due to the intensified plastic flow within the billet volume. The application of ECAP to cast material also resulted in partial defect closure; however, it required additional preparation steps. Studies were also conducted to examine the effect of temperature on the stability of the obtained UFG structure and its mechanical properties. It was revealed that the structure remains stable and maintains high mechanical performance up to 400 °C. At higher temperatures, signs of recrystallization and grain growth were observed, accompanied by a decrease in hardness and strength.

Thus, as a result of the conducted research:

– A technology for forming an ultrafine-grained (UFG) structure in the Zr–1%Nb alloy by the radial-shear rolling (RSR) method has been developed and experimentally verified.

– The feasibility of producing long-length billets with a gradient structure and a high degree of grain refinement has been confirmed.

– A correlation between the microstructure, crystallographic texture, and mechanical properties has been established.

– High-detailed maps of texture and microstructure have been obtained, including the determination of Kearns parameters.

– The high radiation resistance of ultrafine-grained zirconium after ion irradiation has been confirmed.

– The scalability and industrial applicability of the radial-shear rolling (RSR) technology have been confirmed.

– The scientific novelty of the research lies in the systematic approach to studying the radial-shear rolling (RSR) technology for zirconium alloys, encompassing modeling, experimentation, microstructural analysis, mechanical testing, and evaluation of radiation resistance. The work presents original results that have no direct analogs in the available scientific literature.

– The practical significance of the study is confirmed by the potential application of the proposed technology for the industrial production of structural materials used in the cores of next-generation nuclear reactors. The obtained results can be utilized in the development of new fuel assemblies with extended service life and enhanced safety.

Thus, the objectives set forth in the dissertation have been achieved, the research tasks successfully accomplished, and the obtained results represent a valuable contribution to the advancement of materials science and nuclear energy technologies. The work demonstrates a high degree of completeness, internal consistency, scientific validity, and experimental reliability.

Scientific Novelty:

– In this work, finite element computer modeling was employed to investigate the regularities of stress–strain state formation during the radial-shear rolling process of zirconium-based alloys and to analyze the influence of geometric and technological parameters on it.

– An experimental study was conducted with variation of the technological parameters of the radial-shear rolling (RSR) process, and the optimal conditions for obtaining an ultrafine-grained (UFG) structure were determined.

– The entire process of microstructural evolution along the full cross-section was investigated in high detail at all stages of formation under the action of intense shear deformations and vortex metal flow generated by the radial-shear rolling (RSR) method.

– Heavy-ion irradiation of the gradient structure produced by the radial-shear rolling (RSR) method was carried out to simulate fission fragment damage, and the resulting changes in mechanical properties and fine structural evolution were investigated.

Theoretical Significance: The study investigated the feasibility of successfully applying the radial-shear rolling (RSR) method to zirconium alloy E110. The regularities of ultrafine-grained (UFG) structure formation and the evolution of improved mechanical properties in the processed samples were examined and established.

Practical Significance: The research substantiates the potential applicability of the RSR process for the fabrication of high-quality components with enhanced performance characteristics intended for use in the core of nuclear reactors.

CONTRIBUTIONS OF DISERTATION

The dissertation work covers the entire research cycle: from substantiation of the scientific significance and relevance of the topic, theoretical modeling of processes and development of technological modes to full-scale experiments, complex microstructural and mechanical characterization and assessment of radiation resistance of the obtained material.

Based on the results of the conducted research, the following contributions can be identified**.**

Scientific contributions:

1. An original systematic scientific approach to studying the technology of radial-shear rolling as a method of severe plastic deformation of zirconium alloys has been developed and implemented, encompassing numerical modeling, experimental rolling, microstructural analysis, mechanical property evaluation, and radiation-resistance testing. The obtained results are original and have no analogues in the existing scientific literature.
2. The feasibility of successfully applying the Radial-Shear Rolling (RSR) method to the Zr-1%Nb (E110) alloy has been demonstrated. The regularities of ultrafine-grained (UFG) structure formation and evolution, as well as their influence on the mechanical properties of the processed samples, have been established. The obtained data expand the fundamental understanding of the mechanisms of grain-structure formation and texture development in zirconium alloys under RSR.
3. The physical mechanisms responsible for the enhancement of strength and radiation resistance upon reducing the grain size to the ultrafine-grained level have been substantiated. It has been shown that the high density of grain boundaries promotes the formation of a stable structure and improves the overall set of material properties.

Applied Scientific Contributions

A technology for forming an ultrafine-grained structure in zirconium alloys using severe plastic deformation methods—specifically, radial-shear rolling (RSR)—has been developed and experimentally validated, followed by a comprehensive analysis of the structural and performance characteristics of the processed material:

1. A finite-element model of the radial-shear rolling (RSR) process was developed in the DEFORM-3D software. The stress–strain state of the Zr-1%Nb (E110) zirconium alloy billet under conditions of high deformation intensity was analyzed. Optimal rolling parameters—including billet temperature, roll rotation speed, single-pass reduction, and friction coefficient—were determined. The simulation results formed the basis for designing experimental regimes and for model verification.
2. It was experimentally demonstrated that radial-shear rolling, which is characterized by its ability to introduce large plastic strains with a pronounced shear component and vortex-like metal flow within the billet, can be effectively used to obtain an ultrafine-grained structure in the investigated zirconium

alloy. This approach enabled an increase in strength characteristics while maintaining an acceptable level of ductility.

3. The evolution of the microstructure across the entire transverse cross-section of the bars was investigated with high spatial detail at all stages of radial-shear rolling, which involves substantial shear deformation and vortex metal flow. Microstructural analysis was performed using scanning electron microscopy (SEM/EBSD) and transmission electron microscopy (TEM):
    a. The evolution of the microstructure was established, including the distribution of grain sizes, the types of grain boundaries, the presence of substructural elements, and the characteristic features of the resulting texture.
    b. It was determined that the fraction of the ultrafine-grained (UFG) structure in the transverse cross-section of the billet can reach 35–40% of the outer layer, forming a distinct gradient morphology that combines a UFG state in the peripheral region with a submicrocrystalline or recrystallized structure in the central part.
    c. Using EBSD analysis, highly detailed microstructure and texture maps were obtained, grain orientations were determined, and Kearns parameters reflecting the degree of material anisotropy were calculated. It was established that RSR processing produces predominantly a radial–basal texture in the core of the bar and an atypical rolling texture characterized by a dominant axial basal component in the surface layers.
4. The mechanical properties of the RSR-processed bars were determined and evaluated through uniaxial tensile testing and microhardness measurements across the transverse cross-section.
    a. An increase in strength compared to the initial material was established while maintaining sufficient ductility.
    b. A clear correlation between the local microstructure and microhardness was identified, with regions containing a UFG structure exhibiting the highest values.
5. By comparing the results of equal-channel angular pressing (ECAP) — used as a reference method for producing an ultrafine-grained (UFG) structure — with those obtained via radial-shear rolling (RSR), it was established that RSR enables the formation of a metal structure with a comparable degree of grain refinement while requiring fewer processing passes. At the same time, the resulting structure exhibits a gradient character and a specific, potentially advantageous texture. Moreover, RSR demonstrates superior technological scalability.
6. The feasibility of using RSR for processing zirconium ingots with an as-cast structure was investigated. It was established that the RSR method is capable of effectively closing shrinkage and macro-porosity defects due to the intensified plastic flow within the billet volume. The application of ECAP to

the cast structure also demonstrated partial defect closure; however, it requires additional preparatory steps.

7. Radiation damage of the alloy was simulated through heavy-ion irradiation using the DC-60 accelerator. This methodology makes it possible to reproduce effects analogous to those caused by fission fragments in nuclear fuel. It was established that the zirconium alloy with an ultrafine-grained (UFG) structure maintains stable morphology, exhibits moderate radiation-induced hardening without accompanying embrittlement, and preserves a stable Young's modulus, indicating the promising potential of this material for long-term operation in nuclear reactors.
8. The effect of temperature on the stability of the obtained ultrafine-grained (UFG) structure and the mechanical properties was established. It was found that at temperatures up to 400 °C, the structure remains stable and the mechanical properties are retained at a high level. At higher temperatures, signs of recrystallization and grain growth appear, accompanied by a decrease in hardness and strength.

Applied (Practical) Contributions:

1. The feasibility of producing long rods of various diameters from the zirconium alloy using the developed RSR technology has been experimentally confirmed, enabling the fabrication of bars with a gradient structure and a high degree of grain refinement.

The proposed technology is applicable to industrial production of structural materials with improved performance characteristics. The ultrafine-grained structure formed in the surface layers of the billets, combined with the atypical crystallographic texture resulting from RSR, opens new opportunities for creating high-efficiency materials for nuclear energy applications, characterized by enhanced radiation resistance and superior mechanical properties during long-term operation. The obtained data can be used in the development of new manufacturing technologies for fuel cladding tubes with extended service life and improved safety.

PARTICIPATION AND PUBLICATIONS

Scientific Publications on the Dissertation Topic:

1. Arbuz A., Kawalek A., Ozhmegov K., Panin E., Magzhanov M., Lutchenko N., Yurchenko V., *Obtaining an Equiaxed Ultrafine-Grained State of the Longlength Bulk Zirconium Alloy Bars by Extralarge Shear Deformations with a Vortex Metal Flow*, **Materials,** 2023, 16(3), 1062; pp. 1-14; https://doi.org/10.3390/ma16031062; eISSN 1996-1944, Published by MDPI

2. Arbuz A.S., Popov F.E., Panichkin A.V., Kawalek A., Lutchenko N.A., Ozhmegov K. *Using the Radial-Shear Rolling Method for Casted Zirconium Alloy Ingot Structure Improvement*, **Materials,** 2024, 17(20), 5078; pp. 1-17; https://doi.org/10.3390/ma17205078; eISSN 1996-1944, Published by MDPI

3. Lutchenko, N., Yordanova, R., Arbuz, A., *Study of the effect of equal-channel angular pressing on the closure of casting defects in zirconium alloys*, **Journal of Chemical Technology and Metallurgy**, 2025, 60(2), pp. 345–358; ISSN 1314-7471 (print), ISSN 1314-7978 (on line)

4. Alexandr Arbuz, Nikita Lutchenko, Rozina Yordanova, *FEM Method Study of the Advanced ECAP Die Channel and Tool Design*, **Modelling,** 2025, 6(1), 19; pp. 1-14; https://doi.org/10.3390/modelling6010019; eISSN 2673-3951, Published by MDPI

5. Arbuz A., Lutchenko N., Panin E., Lepsibaev A., Magzhanov M., ***A****pplication of the Finite Element Method for Modeling Radial-Shear Rolling of the Zr–1%Nb Alloy*, Vestnik KazNRTU (Kazakh National Research Technical University named after K.I. Satpayev*)*, 2020, No. 5 (141), pp. 701–707; ISSN 1680-9211 **(in Russian)**

6. Lutchenko N.A., Arbuz A.S., Kavalek A.A., Panin E.A., Popov F.E., Magzhanov M.K., *Study of the Influence of Large Shear Deformations and Vortex Metal Flow on the Formation of an Equiaxed Ultrafine-Grained Structure in Zirconium Alloy E110 by the RSR Method,* Foundry Production and Metallurgy, 2023, No. 1, pp. 128–134. https://doi.org/10.21122/1683-6065-2023-1-128-134; ISSN 1683-6065 (Print), ISSN 2414-0406 (Online), **(in Russian)**

The main results of the research were presented and discussed at the following conferences:

1. Arbuz A., Kawalek A., Ozhmegov K., Lutchenko N., Panin E. FEM-simulation of radial-shear rolling of Zr-1%Nb alloy // 6th International conference on recent trends in structural materials (COMAT 2020), – Pilsen, 2020.
2. Panin E., Dikov A., Lutchenko N., Samokhvalov I., Magzhanov M. Arbuz A., FEM simulation of fuel element under loading with the UFG zirconium properties // 3rd International Conference on Functional Materials and Applied Technologies (FMAT-2021), – Harbin, 2020.

3. Arbuz A., Panin E., Kawalek A., Samokhvalov I., Lutchenko N., Magzhanov M. FEM simulation of Zr-1%Nb alloy processing by radial-shear rolling // The 7th Nuclear Materials Conference 2022 (NuMat-2022), – Gent, 2020.
4. Magzhanov M.K., Panin E.A., Popov F.E., Lutchenko N.A., Kuis D.V., Arbuz A.S. Modeling of Vortex Plastic Flow of Zirconium Alloy E110 Based on Plastometric Studies (Modelirovanie vykhrevogo plasticheskogo techeniya tsirkonievogo splava E110 na osnove plastometricheskikh issledovaniy) // XXXV International Scientific Conference “Mathematical Methods in Engineering and Technology – MMTT-35”, Minsk, 2022.
5. Lutchenko N.A., Arbuz A.S., Popov F.E., Samokhvalov I.A. FEM-simulation analysis of spherical cavity ecap design at different channel angles // 32nd International Conference on Metallurgy and materials «Metal 2023». – Brno,2023. - P223-227
6. N. Lutchenko, A. Arbuz, R. Yordanova, Construction and analysis of stress-strain deformation curves of Zr-1%Nb alloy obtained under uniaxial compression, XXII Scientific Poster Session for Young Scientists, Doctoral Students, and Students, UCTM, Sofia, June 20, 2025, p. 62, ISSN 3033-0769
7. N. Lutchenko, A. Arbuz, R. Yordanova, S. Yankova, B. Yankov, Investigation of the influence of temperature-speed deformation conditions on the properties of Zr-1%Nb alloy during uniaxial compression testing, International Conference, "Non-Destructive Testing Days," June 9-13, 2025, Sozopol, Bulgaria
8. A. S. Arbuz, N. A. Lutchenko, F. E. Popov, S. N. Lezhnev, I. E. Volokitina, Application of radial-shear rolling to improve the microstructure of zirconium alloys, XI International Conference Semipalatinsk Test Site: Legacy and Prospects for the Development of Scientific and Technical Potential, 6–10 October 2025, Kurchatov, Kazakhstan

Relation of the dissertation work to research programs:

1. Research funded by the Ministry of Science and Higher Education of the republic of Kazakhstan – «Development of production technology and study of prospect for the use ultrafine-grained zirconium with improved mechanical properties and increased radiation resistance in nuclear energy»; Grant № AP08052429
2. Research funded by the Ministry of Science and Higher Education of the republic of Kazakhstan – «Research & Development new technology for the production of high-quality fuel rod plugs from substandard parts of ingots for nuclear engineering»; Grant № AP14871811
3. Contract with Scientific Research Sector (SRC) at UCTM No. 403-09/2025 "Investigation of the influence of temperature and strain rate on the properties of Zr-1%Nb alloy in uniaxial compression testing", 2025, contract manager Prof. Dr. Eng. Rosina Yordanova